Human pluripotent stem cell–derived erythropoietin-producing cells ameliorate renal anemia in mice

AUTHOR(S):

Hitomi, Hirofumi; Kasahara, Tomoko; Katagiri, Naoko; Hoshina, Azusa; Mae, Shin-Ichi; Kotaka, Maki; Toyohara, Takafumi; ... Nakahata, Tatsutoshi; Nishiyama, Akira; Osafune, Kenji

CITATION:

Hitomi, Hirofumi ...[et al]. Human pluripotent stem cell–derived erythropoietin-producing cells ameliorate renal anemia in mice. Science Translational Medicine 2017, 9(409): eaaj2300.

ISSUE DATE:

2017-09-27

URL:

http://hdl.handle.net/2433/227425

Human pluripotent stem cell-derived erythropoietin-producing cells improve renal anemia in mice

Hirofumi Hitomi[1,2], Tomoko Kasahara[1], Naoko Katagiri[1], Azusa Hoshina[1], Shin-Ichi Mae[1], Maki Kotaka[1], Takafumi Toyohara[1], Asadur Rahman[2], Daisuke Nakano[2], Akira Niwa[3], Megumu K. Saito[3], Tatsutoshi Nakahata[3], Akira Nishiyama[2], Kenji Osafune[1]*

[1]Department of Cell Growth and Differentiation, Center for iPS Cell Research and Application (CiRA), Kyoto University, Kyoto, Japan.

[2]Department of Pharmacology, Faculty of Medicine, Kagawa University, Kagawa, Japan.

[3]Department of Clinical Application, Center for iPS Cell Research and Application (CiRA), Kyoto University, Kyoto, Japan.

Corresponding author E-mail: osafu@cira.kyoto-u.ac.jp

Overline: Kidney Disease

One Sentence Summary:
iPSC-derived cells secrete functional erythropoietin in a physiological manner and ameliorate renal anemia in a mouse model.

Cell therapy for renal anemia using iPSCs

Erythropoietin dysregulation is a hallmark of renal anemia. Although recombinant erythropoietin treatment is beneficial and safe, more physiological therapies are required. Hitomi et al. developed a differentiation protocol for erythropoietin-producing cells from human and mouse iPSCs/ESCs. These cells produced and secreted functional erythropoietin protein in a hypoxia-dependent manner. Transplantation of these cells into a mouse model improved renal anemia. From the perspective of basic research, erythropoietin cells may be a useful tool for investigating the molecular mechanisms of erythropoietin production and secretion. From the perspective of clinical research, these results may provide a physiological therapeutic agent for renal anemia.

Abstract

The production of erythropoietin (EPO), a principal hormone for the hematopoietic system, by the kidneys is reduced in patients with chronic kidney disease (CKD), eventually resulting in severe anemia. Although recombinant human EPO treatment improves anemia in patients with CKD, returning to full red blood cell production without fluctuations does not always occur. In this study, we established a method to generate EPO-producing cells from human induced pluripotent stem cells (hiPSCs) by modifying previously reported hepatic differentiation protocols. These cells showed increased EPO expression and secretion in response to low oxygen conditions, prolyl hydroxylase domain-containing enzymes inhibitors and insulin-like growth factor-1. The EPO protein secreted from hiPSC-derived EPO-producing (hiPSC-EPO) cells induced the erythropoietic differentiation of human umbilical cord blood progenitor cells *in vitro*. Furthermore, transplantation of hiPSC-EPO cells into mice with CKD induced by adenine treatment improved renal anemia. Thus, hiPSC-EPO cells may be a useful tool for clarifying the mechanisms of EPO production and may be useful as a therapeutic strategy for treating renal anemia.

Introduction

Erythropoietin (EPO), a potent regulator of erythropoiesis, is secreted by the kidney and liver. The kidney is the major site of EPO production in adults, and the liver is the primary organ of EPO production in the fetal and early neonatal periods, but EPO is produced by the adult liver in states of severe anemia (*1*, *2*). EPO production is reduced in patients with chronic kidney disease (CKD), eventually resulting in renal anemia. Treatment with recombinant human EPO (rhEPO) improves the control of renal anemia compared to conventional therapies such as blood transfusions that have been associated with viral infections and iatrogenic hemosiderosis. However, although rhEPO is relatively safe, the requirement for infusions 1-3 times/week makes it difficult to return to physiological control of red blood cell production (*3*). In addition, the total cost of rhEPO is increasing due to the increasing number of CKD patients, and patients with anemia secondary to chronic diseases may not respond well to rhEPO (*4*). Finally, very rare cases of severe anemia caused by germline mutations in EPO (*5*) or by anti-rhEPO autoantibodies following the administration of rhEPO have also been reported (*6*, *7*). Therefore, new physiological therapies for renal anemia are required.

The differentiation of induced pluripotent stem cells (iPSCs) (*8*, *9*) and embryonic stem cells (ESCs) (*10*), which have unlimited self-renewal capability and the potential to differentiate into any cell type in the body, provides promising cell sources for regenerative medicine. The somatic cell types differentiated from these stem cells have the potential for clinical applications and practical use, including cell therapy, drug screening, toxicology and disease modeling. Although vigorous efforts have been made to generate multiple somatic cell types from these stem cells, the directed differentiation of EPO-producing cells (EPO cells) from iPSCs or ESCs has not yet been achieved. EPO cells were originally identified in mouse kidney (*11*), but the development

of culture methods for these cells has proved difficult. For this reason, we considered cultured EPO cells derived from iPSCs or ESCs for both basic and clinical applications. One basic research application of iPSC/ESC-derived EPO cells is to clarify the mechanisms of EPO production and secretion, given that EPO cells isolated from the kidney or liver are not readily available. Clinical applications of iPSC- or ESC-derived EPO cells include transplanting these cells as a cell therapy for treating renal anemia.

In the present study, we aimed to establish a differentiation method for producing EPO cells from human iPSCs (hiPSCs) and ESCs (hESCs). We modified previously reported differentiation protocols for hepatic lineages and generated cells expressing EPO from mouse and human iPSCs and ESCs. These cells could physiologically regulate EPO production, as evidenced by increased EPO expression in response to low oxygen conditions. EPO protein secreted by hiPSC-derived EPO (hiPSC-EPO) cells induced the differentiation of human umbilical cord blood progenitor cells into erythropoietic cells *in vitro*. Furthermore, we confirmed that the transplantation of hiPSC-EPO cells into a mouse model of CKD improved renal anemia.

Results

Generation of EPO-producing cells from human iPSCs/ESCs

Given that the liver is the primary organ of EPO production in the fetal stage, we examined *EPO* mRNA expression in human fetal liver. In particular, we measured *EPO* mRNA expression in various human tissues including human fetal liver and adult kidney (Figure 1A). To confirm EPO expression during normal development, we examined EPO expression in embryonic day (E) 12.5 mouse fetal liver by immunostaining (Figure 1B). The results showed that almost all hepatoblasts were positively stained for both α-fetoprotein (AFP) and EPO protein, suggesting that most or all hepatocytes were derived from EPO-producing hepatoblasts.

We thus aimed to generate EPO cells from the hiPSC 253G4 cell line (*12*) by modifying previously reported protocols for hepatic lineage differentiation (Figure S1) (*13*, *14*). As a result, hepatic lineage cells derived from hiPSCs expressed *EPO* mRNA at Stage 2, and the expression disappeared at Stage 3 (Figure 1C). The expression of both *SOX17* and *AFP* was also detected in Stage 2 cells, confirming that the differentiated cells obtained in the hepatic differentiation step (Stage 2) but not the maturation step (Stage 3) mainly produced EPO. We next examined the time course of *EPO* mRNA expression in Stage 2 cells and found that the expression gradually increased with statistical significance on culture day 8 (55.49 ± 6.22 fold increase on day 8 vs. day 0, $p < 0.05$; Figure 1D). Consistent with the results of the qRT-PCR analysis, the increase in EPO protein expression became statistically significant on day 12 (3.42 ± 0.53 fold increase vs. day 0, $p < 0.05$) according to Western blot analysis (Figure 1E). The EPO protein expression was also confirmed by immunostaining, which showed signals in the cytoplasm of the induced cells at Stage 2 and confirmed that the EPO cells were also positive for the hepatic lineage marker, AFP (Figure 1F). AFP and another hepatic lineage marker albumin along with the endoderm markers,

hepatocyte nuclear factor (HNF)-1β, HNF-4, Sal-like protein 4 (SALL4), GATA4 and cytokeratin (CK) 19, were expressed in almost all hiPSC cells producing EPO (hiPSC-EPO) (Figure S2). In addition, EPO expression as analyzed by immunostaining was similar across the hiPSC-EPO cell population (Figure S2). Ultrastructural observations using transmission electron microscopy revealed that EPO cells contained numerous vesicles in the cytoplasm, but these were less dense than in the mouse fetal liver (Figure 1G). Next, we examined EPO protein secretion by hiPSC-EPO cells into the culture medium. The concentration of EPO protein measured using enzyme-linked immunosorbent assay (ELISA) showed a statistically significant increase in the culture medium of hiPSC-EPO cells at Stage 2 after 8 days of culture (0.20 ± 0.05 ng/mL on day 8 vs. day 0, $p < 0.05$; Figure 1H).

Different hiPSC/ESC lines vary in their differentiation potential (*14, 15*). We thus confirmed the generation of EPO cells from multiple hiPSC/ESC lines using our differentiation protocol, including eight hiPSC lines (201B6, 201B7, 253G1, 253G4, 585A1, 604A3, 606A1 and 606B1) (*8, 12, 14*) and two hESC lines (KhES3 and H9) (*10, 16*). The results suggested that EPO cells can be differentiated from multiple hiPSC/ESC lines using our modified hepatic differentiation protocol, although the *EPO* mRNA expression was variable among the cell lines (Figure 1I). We then investigated the correlation of EPO mRNA expression and protein secretion and mRNA expression of the hepatoblast markers AFP and DLK1 in the 253G4, 585A1 and KhES3 cell lines. EPO mRNA expression and protein secretion correlated with the expression of hepatoblast markers in the 253G4 and 585A1 cell lines, but not when the 585A1 and KhES3 cell lines were compared, suggesting that both the differentiation potential of hiPSC/ESC-EPO cells and EPO production and secretion capacity were variable among the cell lines (Figure S3).

hiPSC-EPO cells show long-term proliferative and EPO-producing capacity *in vitro*

We evaluated the long-term proliferation and EPO-producing capacity of hiPSC-EPO cells *in vitro*. The number of hiPSC-EPO cells increased in a time-dependent manner (Figure 2A), and some hiPSC-EPO cells at Stage 2 on day 12 of culture stained positively for the cell proliferation marker Ki67 (Figure 2B). By developing an *in vitro* maintenance culture method for hiPSC-EPO cells using Stage 2 culture medium and gentle cell passaging with Accutase treatment, we could increase the number of cells about 1,000 times after 10 cell passages in 70 days (Figure 2C), during which time both EPO mRNA expression and protein secretion were maintained (Figures 2D and 2E). These results suggest that hiPSC-EPO cells have long-term proliferative and EPO-producing capacity *in vitro.*

Generation of EPO-producing cells from mouse iPSCs/ESCs

We next examined whether mouse iPSCs/ESCs (miPSCs/ESCs) could also be induced to differentiate into EPO cells. Modifying our differentiation method for driving hiPSCs to become EPO cells, we developed a differentiation protocol for obtaining EPO cells from miPSCs/ESCs (Figure S4). qRT-PCR analyses showed that the miPSC cell line 492B-4 treated with our differentiation protocol expressed *Epo* mRNA during Stage 2 of development, and that the expression became statistically significant on culture day 10 (5.88 ± 1.02 fold increase vs. day 0, $p < 0.05$; Figure 3A). We subsequently confirmed that our differentiation protocol to induce EPO cells also worked with the mESC D3 cell line (Figure 3B). EPO protein secretion into the culture medium was also confirmed by ELISA, which showed that the protein concentration increased in a time-dependent manner (Figure 3C). These results indicate that our differentiation protocol could be used to generate EPO cells from both mouse and human iPSCs/ESCs.

IGF-1 treatment augments EPO production and secretion in hiPSC-EPO cells

In order to increase EPO production and improve the differentiation efficiency of EPO cells from hiPSCs/ESCs, we evaluated the effects of various growth factors and chemicals on *EPO* expression during Stage 2 culture. The screening results for 46 different factors showed that the addition of human insulin-like growth factor-1 (IGF-1) most potently augmented *EPO* mRNA expression (Figure S5). We next compared the effects of IGF-1 on *EPO* expression with that induced by related factors, such as IGF-2 and insulin (Figure 4A). IGF-1 treatment at 100 ng/mL increased *EPO* gene expression around 6-fold compared to that observed in controls treated with no additional factors, whereas the same concentration of IGF-2 or insulin had little or no effect. Western blot analyses confirmed that Stage 2 hiPSC-EPO cells expressed the IGF-1 receptor (Figure 4B). We then examined the dose response and time course of EPO gene expression and protein secretion in the culture medium following IGF-1 treatment. Both EPO gene expression and protein secretion were augmented by IGF-1 treatment in a dose-dependent and time-dependent manner (Figures 4C-4F). IGF-1 treatment at 100 ng/mL resulted in a significant increase in *EPO* mRNA expression after four days (82.14 ± 10.86 fold increase on day 4 vs. day 0 before IGF-1 treatment, $p < 0.05$) and EPO protein secretion after eight days (0.19 ± 0.02 ng/mL on day 8, $p < 0.05$), which continued to increase up to day 12. Neither *AFP* nor *ALBUMIN* mRNA expression was significantly changed by IGF-1 treatment, excluding the possibility that IGF-1 altered the differentiation state of the hiPSC-EPO cells (Figures 4G and 4H). These results indicate that IGF-1 treatment promoted EPO production by hiPSC-EPO cells.

Hypoxia augments EPO production by hiPSC-EPO cells

It has been reported that EPO production is regulated by oxygen concentrations through hypoxia-inducible factors (HIFs) and their regulators, prolyl hydroxylase domain-containing enzymes (PHDs) (*17*). We examined whether this was also the case with hiPSC-EPO cells and evaluated the effects of hypoxia on EPO gene expression and protein secretion in hiPSC-EPO cells (Figures 5A, 5B). The results showed that both EPO mRNA expression and protein secretion gradually increased even under normoxic condition (21% oxygen) for the first 8 days of Stage 2 development in parallel with the *AFP* and *ALBUMIN* mRNA expression (Figures 5C and 5D), indicating that the differentiation or maturation of hiPSC-EPO cells proceeded to some extent during these 8 days. Nevertheless, hypoxia (1% oxygen) increased *EPO* mRNA expression and EPO protein concentration in the culture medium more than under normoxic conditions, with statistically significant differences in *EPO* mRNA expression on day 6 and in EPO protein secretion on day 10 ($p < 0.05$; Figures 5A and 5B). In addition, the sensitivity of hiPSC-EPO cells to the hypoxic conditions was evaluated. Compared to the normoxic condition (21% oxygen), two hypoxic conditions (5% and 1% oxygen) augmented EPO mRNA expression and protein secretion dose-dependently (Figures S6A and S6B). In contrast, hypoxia did not significantly alter *AFP* or *ALBUMIN* mRNA expression, excluding the possibility that hypoxia affected the differentiation state of the hiPSC-EPO cells (Figures 5C, 5D). These results suggest that hiPSC-EPO cells are functionally similar to EPO cells *in vivo* in that they produce and secrete EPO in response to the oxygen concentration.

We then evaluated the effects of three PHD inhibitors: dimethyloxaloylglycine (DMOG), deferoxamine (DFO) and FG4592 (*18*). First, we confirmed the expression of HIF subunits. *HIF-1α, -2α, -3α, -1β* and *-2β* mRNA expression was detected in both hiPSC-EPO cells and HepG2 cells, an immortalized human cell line that secretes EPO protein in an oxygen-dependent manner

(Figure S6C). We also confirmed the protein expression of HIF-1α and -2α by immunostaining in hiPSC-EPO cells (Figure S6D). In addition, both hiPSC-EPO cells and HepG2 cells expressed *PHD1*, *PHD2* and *PHD3* mRNAs, sharing the expression of the same HIF and PHD genes with human fetal liver (Figure S6C). In hiPSC-EPO cells, DFO and FG4592 significantly augmented EPO production in a dose-dependent manner, whereas DMOG did not (Figures 5E, 5F, S6E and S6F). Furthermore, an inhibitor of HIF-1 dimerization, Acriflavine, attenuated EPO production in hiPSC-EPO cells (Figure 5G). In contrast, in HepG2 cells, DFO and DMOG augmented EPO production, but FG4592 did not (Figures 5E, 5F). We also confirmed that hypoxic culture conditions stabilized HIF-1α and -2α, as evidenced by the augmentation of nuclear signals revealed using anti-HIF-1α and -2α immunostaining of hiPSC-EPO and HepG2 cells (Figure 5H). IGF-1 treatment also stabilized HIF-1α and -2α and increased EPO expression (Figures 4D, S6G and S6H). These data suggest that hiPSC-EPO cells produce EPO via the HIF-PHD pathway and that hiPSC-EPO and HepG2 cells may use different regulatory machineries to express EPO.

EPO protein produced by hiPSC-EPO cells shows erythropoietic activity *in vitro*

EPO is essential for erythropoiesis and is the primary regulator of this process. In order to evaluate the erythropoietic potential of human EPO protein produced by hiPSC-EPO cells (hiPSC-EPO protein), we performed clonogenic hematopoietic progenitor cell assays in methylcellulose with purified and concentrated hiPSC-EPO protein (Figure 6A). Similar to observations for rhEPO, treatment with hiPSC-EPO protein significantly increased the number of erythroid burst-forming unit colonies (BFU-E, Figure 6B; 7.33 ± 1.20 colonies with 2.8 ng/mL hiPSC-EPO protein, $n = 3$, vs. 2.00 ± 0.00 colonies without EPO treatment, $n = 3$, $p < 0.05$), but not other types of colonies, such as granulocyte-macrophage colony-forming units (CFU-GM; 9.33

± 1.45 colonies with 2.8 ng/mL hiPSC-EPO protein, n = 3, vs. 6.00 ± 1.16 colonies without EPO treatment, n = 3, $p > 0.05$), differentiated from cord blood $CD34^+$ hematopoietic progenitor cells (Figure 6C, Table S1). The efficiency of BFU-E formation induced by hiPSC-EPO protein was similar to that achieved with rhEPO protein (6.67 ± 0.33 colonies with 2.8 ng/mL rhEPO protein, n = 3, $p > 0.05$). However, the erythropoietic effects of the hiPSC-EPO protein (2.8 ng/mL) were markedly suppressed by adding human EPO-specific antibodies (Figure 6D, Table S1). These results suggest that hiPSC-EPO cells secrete functional EPO protein that can stimulate erythropoiesis to a similar extent as conventional rhEPO protein.

EPO protein produced by hiPSC-EPO cells shows erythropoietic activity *in vivo*

A renal anemia mouse model was developed using adenine treatment of C57BL/6 mice (*19*, *20*). Oral gavage of adenine (50 mg/kg body weight daily for 4 weeks) decreased hematocrit and hemoglobin concentration. The mice were then further treated after dividing them into the following five groups: group 1, no adenine treatment (control; n = 6); group 2, rhEPO 28 ng, subcutaneous injection (s.c.) (n = 10); group 3, rhEPO 0.56 ng, s.c. (n = 10); group 4, hiPSC-EPO protein 0.56 ng, s.c. (n = 10); and group 5, saline, s.c. (n = 10). Notably, the subcutaneous injection of rhEPO and hiPSC-EPO protein into the mice for four weeks resulted in recovery of both the hematocrit (normal range in C57BL/6 mice, 36.8 – 52.7%; 39.78 ± 0.51% with hiPSC-EPO protein, n = 10, vs. 33.85 ± 0.52% with saline, n = 10, $p < 0.05$; Figures 7A and 7B) and hemoglobin concentration (normal range in C57BL/6 mice, 11.0 – 15.2 g/dL; 11.40 ± 0.16 g/dL with hiPSC-EPO protein vs. 9.52 ± 0.27 g/dL with saline, $p < 0.05$; Figure 7C) (*21*) to within the normal range. However, this treatment did not increase the number of white blood cells or platelets (Figure 7D), suggesting that hiPSC-EPO protein induces the differentiation of only erythrocyte progenitor cells.

The adenine-treated mice did not show any significant changes in mean corpuscular volume or mean corpuscular hemoglobin concentration (Figure 7E) or body weight (Figure S7A) after four weeks of treatment with rhEPO or hiPSC-EPO protein. Whereas the mouse EPO concentrations measured using ELISA were not affected by human EPO treatment in the adenine-treated mice (Figure 7F), the human EPO concentrations increased after treatment with rhEPO (28 ng) or hiPSC-EPO protein (0.56 ng), suggesting that the mouse renal anemia was improved by treatment with human EPO protein (Figure 7G). We also confirmed that both hiPSC-EPO protein and rhEPO improved renal anemia in a dose-dependent manner (Figure S7B). The efficiency of renal anemia recovery was calculated based on the increase in hematocrit per week. Treatment with hiPSC-EPO protein more efficiently improved the anemic state than did rhEPO treatment (3.46 ± 0.47%/week with hiPSC-EPO protein 0.56 ng vs. 1.00 ± 0.52%/week with rhEPO 0.56 ng; Figure 7H). To elucidate the molecular mechanisms responsible, we measured the glycosylation pattern of hiPSC-EPO protein by lectin microarray analysis (Figure 7I). Although the glycosylation pattern resembled that of two clinically available rhEPOs (epoetin-α and epoetin-β), the glycosylation of hiPSC-EPO protein was more complicated, as evidenced by its reactivity with numerous lectins. Because glycosylation modulates the efficacy and degradation of EPO (*22*), we also compared half-lives *in vivo* and found that hiPSC-EPO had a slightly longer half-life than did epoetin-β in mice, although the difference may not be clinically significant (Figure 7J). These data suggest that EPO protein produced by hiPSC-EPO cells was capable of inducing erythropoiesis *in vivo* as well as *in vitro* and that different glycosylation patterns may help to explain why hiPSC-EPO protein induced a slightly greater hematocrit in mice with renal anemia mice than did rhEPO. However, we should note that there may be no biological difference between the two EPO proteins, because increased doses of rhEPO resulted in bioequivalence with hiPSC-EPO protein (Figure S7B).

Transplantation of hiPSC-EPO cells improves renal anemia in mice

Immunodeficient (NOD.CB17-*Prkdc*^{scid}/J) mice were treated with adenine by oral gavage (50 mg/kg body weight daily for 5 weeks) to induce renal anemia. In order to examine the feasibility of hiPSC-based cell therapy for treating renal anemia, 20 aggregates of hiPSC-EPO cells (5.0×10^5 cells/aggregate) were transplanted under the kidney subcapsules of the anemic mice. Notably, transplantation of hiPSC-EPO cells significantly improved renal anemia after four weeks compared with saline treatment (hematocrit: normal range in NOD.CB17-*Prkdc*^{scid}/J mice, 42.3 – 48.1%; 42.56 ± 1.74% with hiPSC-EPO cells, n = 6, vs. 34.60 ± 5.23% with saline, n = 6, $p < 0.05$; Figure 8A) (*21*). The human EPO concentration in the host mouse serum at four weeks after transplantation was detectable using ELISA and was significantly increased in the mice that underwent transplantation with hiPSC-EPO cells (1.42 ± 0.23 ng/mL with hiPSC-EPO cells, n = 6, vs. 0.07 ± 0.02 ng/mL with saline, n = 6, $p < 0.05$; Figure 8B). Importantly, mice with renal anemia transplanted with hiPSC-EPO cells did not develop polycythemia during the observation period (for up to 28 weeks after transplantation), and their hematocrit remained within the normal range. In contrast, renal anemia persisted in adenine-treated mice that did not undergo transplantation (46.40 ± 3.49% with hiPSC-EPO cells, n = 4, vs. 37.23 ± 2.86% with saline, n = 4, at 28 weeks after transplantation, $p < 0.05$; Figure 8C). In addition, human EPO protein in mouse serum was also detectable for up to 28 weeks after transplantation (Figure 8D). We performed histological analyses of the hiPSC-EPO cell aggregates injected under the renal subcapsule of immunodeficient mice. Hematoxylin and eosin staining revealed structures consisting of homogenous cells in the grafts (Figure 8E). Immunohistochemical analysis revealed that the transplanted hiPSC-EPO cell aggregates maintained EPO expression in the subcapsule of host

mouse kidneys for at least 28 weeks after transplantation (Figure 8E). While AFP expression was decreased 8 weeks after transplantation, albumin expression was detectable for 28 weeks after transplantation (Figure 8E). Blood vessel-like tubular structures were found inside the grafts and contained red blood cells (Figure 8F). The new vasculature derived from host mice was confirmed by the expression of mouse CD31/platelet endothelial cell adhesion molecule-1 (PECAM-1), indicating that mouse host blood vessels may have supplied nutrition and oxygen to the grafts. EPO secretion from transplanted hiPSC-EPO cells after phlebotomy was evaluated (Figure 8G). We found that moderate phlebotomy (with the hematocrit decreased from 44% to 34%) in the group transplanted with hiPSC-EPO cell aggregates resulted in an increase in circulating human EPO, but this did not occur in control untransplanted mice (Figure 8G). These data indicate that hiPSC-EPO cells can survive in host mice with renal anemia, subsequently secrete functional human EPO protein and improve renal anemia in the mice.

Discussion

Although rhEPO treatment is beneficial for CKD patients with renal anemia, several problems remain to be addressed. First, the increasing number of CKD patients is expanding the demand for rhEPO treatment, which in turn increases the total cost of this therapy. Second, it is difficult to physiologically control renal anemia using rhEPO treatment. The intermittent administration of rhEPO causes fluctuations in hemoglobin concentrations (*3*), which is associated with an increased incidence of cardiovascular events (*23*). In addition, the target hemoglobin concentration for rhEPO treatment remains controversial, and hemoglobin concentrations in most patients are lower than those observed in healthy subjects (*24*). The physiological control of renal anemia based on a stable, normal range of hemoglobin concentrations may help in the treatment of CKD patients.

hiPSCs/ESCs are potential cell sources for regenerative medicine. In this study, we generated EPO-producing cells from human and mouse iPSCs/ESCs. These cells expressed EPO mRNA and protein and increased the production and secretion of EPO protein in response to low oxygen conditions. Importantly, the secreted EPO protein induced the erythropoietic differentiation of umbilical cord blood $CD34^+$ hematopoietic cells *in vitro* and improved renal anemia in adenine-treated immunodeficient mice *in vivo*. Furthermore, the transplantation of hiPSC-EPO cells reversed renal anemia, with a return to the normal range of hematocrit in immunodeficient mice. Therefore, EPO cells generated from hiPSCs/ESCs may be useful as a cell therapy for treating renal anemia.

rhEPO treatment is associated with a very rare side effect of severe anemia due to the generation of anti-rhEPO autoantibodies (*6*). Although further studies are needed to clarify the immunological effects of transplanted hiPSC-EPO cells, the cell types generated from a patient's

own iPSCs may provide a safer cell therapy in terms of the immune response. Moreover, we confirmed that hiPSC-EPO cells secreted functional EPO protein for at least 70 days using regular *in vitro* culture conditions. In addition, hiPSC-EPO cells have the potential to survive long-term (28 weeks) after transplantation in the body.

In addition to their application for clinical use, hiPSC/ESC-derived EPO-producing cells will be valuable for basic research. Although much is known about the possible mechanisms of EPO production and secretion, such as the involvement of HIF-2α (*17*), the detailed molecular mechanisms have not yet been fully elucidated due to the limited access to isolated and cultured EPO-producing cells, especially human cells. EPO cells have been identified in the peritubular interstitial space in mouse kidneys (*11*). Moreover, EPO cells were recently isolated from primary cultures of human (*25*) and mouse kidneys (*26*). These cells exhibited gene expression and protein secretion of EPO in an oxygen-dependent manner, suggesting that EPO cells removed from the kidneys can be used to investigate the molecular mechanisms of human EPO production. However, it is difficult to obtain an adequate amount of EPO cells, since access to human kidney specimens is limited. In addition, primary cultured cells isolated from normal human tissues are often difficult to expand *in vitro* long-term . HepG2 cells are widely used to investigate EPO production (*27*, *28*), however, since they are derived from hepatoma tissues, EPO production and secretion may differ from that observed in healthy, non-tumor cells. In the current study, hypoxia activated EPO secretion from the hiPSC-EPO cells, and the secreted EPO protein induced erythropoietic differentiation both *in vitro* and *in vivo*, suggesting that hiPSC-EPO cells may be functionally similar to their *in vivo* counterparts. Given that these EPO cells can be readily derived from human and mouse iPSCs/ESCs and display robust *in vitro* expansion potential, they could be reliable cellular models for investigating the intracellular signaling pathways involved in EPO production and secretion.

Both clinical studies and *in vivo* research using experimental animals have reported that IGF-1 is involved in EPO production and secretion. One clinical study revealed that IGF-1 stimulates EPO secretion from the kidneys of patients with insulin resistance (*29*). On the other hand, the acute injection of IGF-1 negatively controls EPO secretion from mouse kidney (*30*). In addition, IGF-1 suppresses EPO secretion from the kidney, but increases its secretion from the liver (*31*). In the present study, we show that IGF-1 augmented EPO production in hiPSC-EPO cells. Combined, these data suggest that IGF-1 is an important regulatory factor for EPO production and secretion.

Several limitations of our study deserve mention. First, the EPO cells in our study were generated from hiPSCs/ESCs through hepatic lineage differentiation. The liver is a major organ of EPO production in the fetal and early neonatal periods. Although EPO production shifts to the kidney in late gestation and adulthood (*32*), previous studies have reported that EPO production by the adult liver can be induced under anemic or hypoxic conditions (*1, 2, 33*). Nevertheless, methods that induce hiPSCs/ESCs into becoming EPO-producing cells via differentiation through the kidney lineage would be helpful for elucidating the mechanisms of EPO production, especially considering that gene regulation is different between mouse kidney and liver (*34*). It has recently been reported that EPO-producing fibroblasts in normal adult mouse kidney had originated from myelin protein zero-Cre lineage-labeled extrarenal cells, which entered the embryonic kidney on embryonic day (E)13.5 (*35*). As myelin protein zero is expressed in migrating neural crest cells in early embryonic stages, the origin of EPO cells in the kidney may be the neural crest. Therefore, differentiation methods that drive hiPSCs into the neural crest lineage and then into EPO cells could provide insights into kidney-derived EPO production.

Second, the mechanisms underlying the variable responses seen with PHD inhibitors and the different responses between hiPSC-EPO cells and HepG2 cells are still unclear. We evaluated

the effects of three different PHD inhibitors (DMOG, DFO and FG4592) on EPO expression and secretion. Previous studies reported that these PHD inhibitors induced different responses in the expression or function of HIF-PHD pathway molecules and their biological effects (*36, 37*). Furthermore, PHD inhibitors have variable selectivity and inhibitory effects on both cell types, such as liver cell and retina cells, and PHD subtypes, such as PHD1, PHD2 and PHD3 (*37, 38*). Taken together, these differences among PHD inhibitors may at least partly explain the variable responses observed between hiPSC-EPO cells and HepG2 cells. Nevertheless, a recent report indicated that FG4592 has more efficient and broader inhibitory effects on various cell types compared to DMOG (*37*); several clinical trials are using FG4592 (*39, 40*). The present findings that FG4592 augmented EPO production only in hiPSC-EPO cells, but not HepG2 cells, suggest that hiPSC-EPO cells may provide a good model for screening PHD inhibitors for their effects on renal anemia.

One final limitation of our study is that a large number of hiPSC-EPO cells need to be used. At the beginning of this study, we decided on the cell number for transplantation based on EPO secretion *in vitro*. The results of EPO secretion into cell culture medium detected by ELISA indicated that 1 x 10^7 hiPSC-EPO cells secreted approximately 12 ng/day of EPO protein. The findings of *in vivo* dose response experiments (Figure S7B) indicated that this amount of EPO protein was enough to reverse renal anemia. Therefore, we transplanted 1 x 10^7 hiPSC-EPO cells under the left renal subcapsule of each immunodeficient mouse. However, future studies should optimize EPO production capacity and cell number of hiPSC-EPO cells for transplantation. In addition, our data suggest that there was variability in both the differentiation potential and EPO secretion capacity among the different hiPSC/ESC lines. Further optimization and improvement of the differentiation protocol for EPO cells will be required to achieve broad application.

In summary, we successfully generated EPO cells from human and mouse iPSCs/ESCs. These cells produced and secreted functional EPO protein in a hypoxia-dependent manner, and IGF-1 treatment augmented EPO production. From the point of view of basic research, iPSC/ESC-derived EPO cells may be a powerful tool for investigating the molecular mechanisms of EPO production and secretion. hiPSC/ESC-derived EPO-producing cells potentially may provide a useful cell population for cell therapy for the treatment of renal anemia in CKD patients.

Materials and Methods

Study design

The aim of this study was to establish a differentiation method that produces EPO cells from human and mouse iPSCs/ESCs and to evaluate the transplantation of the resulting hiPSC-EPO cells in CKD model mice. EPO production and secretion were evaluated by RT-PCR, immunostaining and ELISA. All mice analyzed in this study were handled and the experimental procedures were performed under the guidelines for the care and use of animals established by Kagawa University and Kyoto University. All animal experiments were approved by the Animal Care and Use Committee for Kagawa University and the Center for iPS Cell Research and Application (CiRA) Animal Experiment Committee. The sample size (n = 6 to 10) for the animal experiments was based on the results of preliminary experiments. Exact numbers for each experiment are described in the figure legends. The investigators were not blinded when evaluating the experiments. The mice were randomly assigned to the treatment and control groups.

Cell culture

hiPSCs (201B6, 201B7, 253G1, 253G4, 585A1, 604A3, 606A1 and 606B1) (*8, 14*) and hESCs (KhES-3 and H9) (*10, 16*) were grown on feeder layers of mitomycin C-treated SNL cells in Primate ES medium (ReproCELL) supplemented with 500 U/mL of penicillin/streptomycin (Thermo Fisher Scientific) and 4 ng/mL of recombinant human basic fibroblast growth factor (bFGF; Wako), as previously described (*41*). The colonies of hiPSCs were dissociated using an enzymatic method with CTK solution consisting of 0.25% trypsin (Thermo Fisher Scientific), 0.1% collagenase IV (Thermo Fisher Scientific), 20% knockout serum replacement (KSR, Thermo Fisher Scientific) and 1 mM $CaCl_2$ in PBS.

miPSCs (492B-4) and mESCs (D3) were maintained on feeder layers of mitomycin C-treated SNL cells in Dulbecco's modified Eagle's medium (DMEM, Nacalai Tesque) supplemented with 15% fetal bovine serum (FBS, Hyclone Laboratory), 500 U/mL of penicillin/streptomycin, 0.1 mM of non-essential amino acids (Thermo Fisher Scientific), 2 mM glutamine (Thermo Fisher Scientific), 0.55 mM 2-mercaptoethanol (Thermo Fisher Scientific) and leukemia inhibitory factor. miPSCs/ESCs were passaged using enzymatic dissociation with 0.25% trypsin/EDTA. HepG2 cells were cultured in DMEM with 10% FBS and 500 U/mL of penicillin/streptomycin.

Differentiation protocols for EPO cells

The differentiation of EPO cells from hiPSCs/ESCs (Figure S1) was performed by modifying previously reported protocols into hepatic lineages (*13, 14, 41*). Colonies of hiPSCs/ESCs grown on a SNL feeder layer were first dissociated according to an enzymatic method with CTK dissociation solution to remove SNL cells. Then, the cells were dissociated to single cells via gentle pipetting after treatment with Accutase (Innovative Cell Technologies) for 20 minutes and seeded on Matrigel-coated plates (BD) at a density of 4.5×10^5 cells/cm^2 with Stage 1 medium containing RPMI 1640 (Nacalai Tesque) supplemented with 500 U/mL of penicillin/streptomycin, B27 supplement (Thermo Fisher Scientific), 100 ng/mL of recombinant human/mouse/rat activin A (R&D Systems) and 1 μM CHIR99021 (Wako). Y-27632 (10 μM, Wako) was added to Stage 1 medium for the first 24 hours. After 24 hours, Stage 1 medium was supplemented with 0.5 mM sodium butyrate (NaB, Sigma-Aldrich) until culture day 3. On day 7, the medium was changed to Stage 2 medium containing Knockout DMEM (Thermo Fisher Scientific) supplemented with 500 U/mL of penicillin/streptomycin, 20% KSR, 1% dimethyl sulfoxide (DMSO), 1 mM L-glutamine, 1% non-essential amino acid and 0.1 mM β-mercaptoethanol. For hepatocyte differentiation, the

cells were shifted to the hepatocyte maturation step after seven days of Stage 2 treatment using incubation with Stage 3 medium containing hepatocyte culture medium (Lonza) supplemented with 10 ng/mL of hepatocyte growth factor (HGF; R&D Systems) and 20 ng/mL of oncostatin M (R&D Systems). For cell passaging, Stage 2 cells were dissociated to single cells via gentle pipetting after treatment with Accutase for 8 minutes and split on Matrigel-coated plates at a ratio of 1:4 with Stage 2 medium containing Y-27632 (10 μM).

The differentiation of EPO cells from miPSCs/ESCs was performed using a similar protocol to that for hiPSCs/ESCs (Figure S4). Briefly, miPSCs/ESCs dissociated to single cells with Accutase treatment were cultured with Stage 1 medium containing RPMI 1640, 500 U/mL of penicillin/streptomycin, B27 supplement, 100 ng/mL of recombinant activin A and 1 μM CHIR99021. After two days, the medium was supplemented with 0.5 mM NaB until day 4. On day 5, the medium was changed to Stage 2 medium.

RT-PCR and real-time quantitative RT-PCR (qRT-PCR)

Total RNA was isolated using the RNeasy kit (Qiagen) according to the manufacturer's recommendations, followed by cDNA synthesis using standard protocols. Briefly, first-strand cDNA was synthesized from 1 μg of total RNA using ReverTra Ace (TOYOBO). The cDNA samples were subjected to PCR amplification using a thermal cycler (Veriti 96-well Thermal Cycler, Thermo Fisher Scientific), and PCR was performed using the Ex-Taq PCR kit (Takara Bio) according to the manufacturer's protocol. The PCR cycles were as follows: for *β-ACTIN*, initial denaturation at 94°C for 2.5 minutes, followed by 25 cycles of 94°C for 30 seconds, 60°C for 1 minute, 72°C for 30 seconds, and final extension at 72°C for 10 minutes. For the other genes, the cycles consisted of initial denaturation at 94°C for 2.5 minutes, followed by 30-40 cycles of

94°C for 30 seconds, 58-62°C for 30 seconds, 72°C for 30 seconds, and final extension at 72°C for 7 minutes. qRT-PCR was performed using the Step One Plus Real-Time PCR System (Thermo Fisher Scientific) and SYBR Green PCR Master Mix (Takara Bio). Denaturation was performed at 95°C for 30 seconds followed by 45 cycles at 95°C for 5 seconds and at 60°C for 30 seconds. The threshold cycle method was used to analyze the data for the gene expression levels and calibrated to those of either housekeeping gene *β-ACTIN* or *GAPDH*. Primer sequences are described in Supplementary Table S2.

Immunostaining

Immunostaining of the cultured cells was carried out as previously described (*41*). Briefly, the cells were fixed with 4% paraformaldehyde/PBS for 20 minutes at 4°C. After washing with PBS, the cells were blocked with 1% normal donkey serum and 3% BSA (Nacalai Tesque)/PBST (PBS/0.25% Triton X-100) for 30 minutes at room temperature. A fetal mouse liver (E12.5) and transplanted aggregates were also fixed with 4% paraformaldehyde/PBS for 20 minutes at 4°C, embedded in paraffin and sectioned into 4-μm slices. The sections were stained with HE staining. The samples were incubated overnight at 4°C with the following primary antibodies: anti-EPO (Santa Cruz Biotechnology), AFP (Sigma-Aldrich), ALBUMIN (Bethyl Laboratories), HNF1β (Santa Cruz Biotechnology), HNF4 (Santa Cruz Biotechnology), SALL4 (Abcam), GATA4 (Santa Cruz Biotechnology), CK19 (Dako), Ki67 (BD), CD31 (Dianova), HIF-1α (Sigma-Aldrich) and HIF-2α (Novus Biologicals). Secondary antibodies (Alexa Fluor antibodies, Thermo Fisher Scientific) were incubated for 30 minutes at room temperature. The stained cells were evaluated using fluorescence microscopy (BZ-9000, Keyence).

Measurement of EPO protein expression

The concentrations of EPO protein in the culture media were measured using ELISA according to the manufacturer's protocol (ALPCO Diagnostics for human EPO and Abnova for mouse EPO). Briefly, the supernatant of the EPO cell cultures was added to a 96-well plate with enzyme-labeled anti-human or anti-mouse EPO antibodies. The plates were incubated for two hours at room temperature. Then, the substrate was added, and the reaction was stopped with 0.5 mM sulfuric acid. The plates were read at 450 nm with a microplate reader (2104 Envision, PerkinElmer), and the concentration of EPO was calculated based on the standard curve of lyophilized synthetic EPO protein.

For the western blot analysis, the EPO protein expression in the cell lysate was measured as previously described (*42*). Briefly, the cells were lysed, and solubilized proteins were isolated via centrifugation and quantified using a Bradford assay. The proteins were separated using SDS-polyacrylamide gel electrophoresis and transferred to nitrocellulose membranes (GE Healthcare). After blocking with Odyssey blocking buffer (LI-COR Biosciences), blots were incubated with anti-EPO (Santa Cruz Biotechnology) or anti-IGF-1 receptor (Cell Signaling Technology) antibodies overnight at 4°C. Blots with embedded Infrared Dye were visualized with the Odyssey Infrared Imaging System (LI-COR Biosciences). In order to confirm the loading of equal amounts of protein, each membrane was reprobed with anti-β-ACTIN antibodies (Sigma-Aldrich). The band intensity was quantified according to immunoblot densitometry using NIH ImageJ software.

Electron microscopy

For observation with transmission electron microscopy, the cells were fixed with 4% formaldehyde and 2% glutaraldehyde in 0.1 M phosphate buffer at 4°C overnight and washed in 0.1 M phosphate

buffer. Then, the cells were refixed with phosphate-buffered 1% OsO_4, dehydrated in a graded series of ethanol and embedded in Luveak 812 (Nacalai Tesque). Thin sections were cut with an EM UC6 ultramicrotome (Leica Microsystems), stained with uranyl acetate and lead citrate and observed using a Hitachi H-7650 electron microscope (Hitachi).

Lectin microarray

The glycosylation patterns of hiPSC-EPO and rhEPO proteins were measured by lectin microarray assays. hiPSC-EPO proteins were concentrated using a centrifugal filter device (Amicon Ultra-15, Millipore) and then purified and isolated with biotin-labeled anti-EPO antibody (Fitzgerald Industries) using Dynabeads MyOne Streptavidin T1 (Thermo Fisher Scientific). Lectin microarray assays were performed by GlycoTechnica as reported previously (*43*).

Clonogenic hematopoietic progenitor assay

Human $CD34^+$ cells were isolated from cord blood via immunomagnetic bead separation (Miltenyi Biotech) according to the manufacturer's instructions. The purity of the isolated $CD34^+$ cells was > 95%, as analyzed using flow cytometry. A total of 1×10^5 $CD34^+$ cells were incubated with rhEPO or hiPSC-EPO protein from hiPSC-EPO cells at 0.28 and 2.8 ng/mL for 2 hours. hiPSC-EPO protein was purified and concentrated using Amicon Ultra-30 (Merck Millipore). Hematopoietic cells were cultured at a low cell density with a concentration of 1×10^4 cells/mL in 35-mm petri dishes (Becton-Dickinson) using 1 mL/dish of MethoCult GF^+ semisolid medium (STEMCELL Technologies) including stem cell factor, thrombopoietin and interleukin 3 (ST3), as previously described (*44*). The number of colonies was counted after 14-21 days of culture, and the colony types (CFU-Mix, BFU-E and CFU-GM) were determined with *in situ* observation using

an inverted microscope according to the criteria described previously (*44*). The abbreviations used for clonogenic progenitor cells are as follows: CFU-Mix, mixed colony-forming units; BFU-E, erythroid burst-forming units; and CFU-GM, granulocyte-macrophage colony-forming units.

Animal experiments

All experimental procedures were performed under the guidelines for the care and use of animals established by Kagawa University and Kyoto University. Six-week-old male C57BL/6 mice (CLEA Japan) were used for the adenine-induced renal anemia model. Renal injury was induced by oral gavage with adenine (50 mg/kg body weight in 0.5% methylcellulose) daily for 4 weeks. The presence of renal anemia was confirmed by measuring Hct and Hb levels and red blood cell count.

One week after the end of adenine treatment, the following five mouse groups were prepared. Group 1: no adenine treatment (control; n = 6); group 2: rhEPO 28 ng, s.c. after adenine treatment (rhEPO 28 ng; n = 10); group 3: rhEPO 0.56 ng, s.c. after adenine treatment (rhEPO 0.56 ng; n = 10); group 4: hiPSC-EPO protein 0.56 ng, s.c. after adenine treatment (hiPSC-EPO protein 0.56 ng; n = 10); and group 5: saline injection after adenine treatment (saline; n = 10). The rhEPO and hiPSC-EPO protein treatments were performed via subcutaneous injection 3 times/week for 4 weeks. For EPO protein dose-response experiments *in vivo*, the following nine mouse groups were prepared. Group 1: no adenine treatment (control; n = 6); group 2: hiPSC-EPO protein 0.56 ng, s.c. after adenine treatment (n = 6); group 3: hiPSC-EPO protein 5.6 ng, s.c. after adenine treatment (n = 6); group 4: hiPSC-EPO protein 14 ng, s.c. after adenine treatment (n = 6); group 5: hiPSC-EPO protein 28 ng, s.c. after adenine treatment (n = 6); group 6: rhEPO 0.56 ng, s.c. after adenine treatment (n = 6); group 7: rhEPO 5.6 ng, s.c. after adenine treatment (n = 6);

group 8: rhEPO 14 ng, s.c. after adenine treatment (n = 6); and group 9: rhEPO 28 ng, s.c. after adenine treatment (n = 6). To measure the half-life of EPO protein, rhEPO and hiPSC-EPO proteins were subcutaneously injected (28 ng) into an adenine-induced renal anemia model. Serum EPO concentrations were measured using ELISA at 1, 6, 24 and 48 hours after injection. The half-life of EPO was evaluated by decreases in serum EPO protein concentration after injection. Blood samples were collected to measure the Hct and Hb levels and EPO protein concentrations. The Hct levels were determined in blood samples withdrawn into glass capillary tubes. The Hb levels were measured using ELISA (Abcam), and the numbers of red blood cells, white blood cells and platelets were counted using a Coulter Counter Multisizer 3 (Beckman-Coulter).

For the transplantation experiments, renal anemia was induced using adenine treatment (50 mg/kg body weight daily for 5 weeks) in immunodeficient mice (NOD.CB17-*Prkdc*^{scid}/J). To prepare the EPO cell aggregates, EPO cells were dissociated to single cells via pipetting after incubation with Accutase for 10 minutes. Then, the EPO cells were split into spindle-shaped bottom low adhesion 96-well plates at a density of 5.0×10^5 cells/well and incubated in Stage 2 medium supplemented with 10 μM Y-27632 for 48 hours. The formation of cellular aggregates was confirmed with microscopic observation. After washing the aggregates with saline, 20 EPO cell aggregates were transplanted into the renal subcapsules of immunodeficient mice with renal anemia. The Hct levels were measured for up to 28 weeks after transplantation. The human EPO concentrations were also measured using ELISA. For immunohistochemistry analysis, mice were sacrificed 2, 4, 8, 16 and 28 weeks after transplantation, and the serial sections of transplanted aggregates were examined by immunostaining. To elucidate the effects of phlebotomy, serum EPO concentrations of control (no transplantation) and hiPSC-EPO cell transplanted mice were measured by Goldenrod animal lancet (MEDIpoint).

Statistical Analysis

Results are expressed as the mean ± SEM. Multiple-group comparisons were made using one-way or two-way analyses of variance (ANOVA) followed by Bonferroni's test. Student's *t*-tests were performed to compare the mean values when the experimental design was comprised of two individual groups. A p value of < 0.05 was considered statistically significant.

Supplementary Materials

References and Notes

1. M. C. Bondurant, M. J. Koury, Anemia induces accumulation of erythropoietin mRNA in the kidney and liver. *Mol Cell Biol* **6**, 2731-2733 (1986).
2. S. de Seigneux, A. K. Lundby, L. Berchtold, A. H. Berg, P. Saudan, C. Lundby, Increased Synthesis of Liver Erythropoietin with CKD. *J Am Soc Nephrol* **27**, 2265-2269 (2016).
3. S. Fishbane, J. S. Berns, Hemoglobin cycling in hemodialysis patients treated with recombinant human erythropoietin. *Kidney Int* **68**, 1337-1343 (2005).
4. O. F. Bamgbola, Pattern of resistance to erythropoietin-stimulating agents in chronic kidney disease. *Kidney Int* **80**, 464-474 (2011).
5. A. R. Kim, J. C. Ulirsch, S. Wilmes, E. Unal, I. Moraga, M. Karakukcu, D. Yuan, S. Kazerounian, N. J. Abdulhay, D. S. King, N. Gupta, S. B. Gabriel, E. S. Lander, T. Patiroglu, A. Ozcan, M. A. Ozdemir, K. C. Garcia, J. Piehler, H. T. Gazda, D. E. Klein, V. G. Sankaran, Functional Selectivity in Cytokine Signaling Revealed Through a Pathogenic EPO Mutation. *Cell* **168**, 1053-1064 e1015 (2017).
6. N. Casadevall, J. Nataf, B. Viron, A. Kolta, J. J. Kiladjian, P. Martin-Dupont, P. Michaud, T. Papo, V. Ugo, I. Teyssandier, B. Varet, P. Mayeux, Pure red-cell aplasia and antierythropoietin antibodies in patients treated with recombinant erythropoietin. *N Engl J Med* **346**, 469-475 (2002).
7. S. K. Lim, P. C. Bee, T. C. Keng, Y. B. Chong, Resolution of epoetin-induced pure red cell aplasia 2 years later, successful re-challenge with continuous erythropoiesis receptor stimulator. *Clin Nephrol* **80**, 227-230 (2013).
8. K. Takahashi, K. Tanabe, M. Ohnuki, M. Narita, T. Ichisaka, K. Tomoda, S. Yamanaka, Induction of pluripotent stem cells from adult human fibroblasts by defined factors. *Cell* **131**, 861-872 (2007).
9. J. Yu, M. A. Vodyanik, K. Smuga-Otto, J. Antosiewicz-Bourget, J. L. Frane, S. Tian, J. Nie, G. A. Jonsdottir, V. Ruotti, R. Stewart, Slukvin, II, J. A. Thomson, Induced pluripotent stem cell lines derived from human somatic cells. *Science* **318**, 1917-1920 (2007).
10. J. A. Thomson, J. Itskovitz-Eldor, S. S. Shapiro, M. A. Waknitz, J. J. Swiergiel, V. S. Marshall, J. M. Jones, Embryonic stem cell lines derived from human blastocysts. *Science* **282**, 1145-1147 (1998).
11. N. Obara, N. Suzuki, K. Kim, T. Nagasawa, S. Imagawa, M. Yamamoto, Repression via the GATA box is essential for tissue-specific erythropoietin gene expression. *Blood* **111**, 5223-5232 (2008).

12. M. Nakagawa, M. Koyanagi, K. Tanabe, K. Takahashi, T. Ichisaka, T. Aoi, K. Okita, Y. Mochiduki, N. Takizawa, S. Yamanaka, Generation of induced pluripotent stem cells without Myc from mouse and human fibroblasts. *Nature biotechnology* **26**, 101-106 (2008).
13. D. C. Hay, D. Zhao, J. Fletcher, Z. A. Hewitt, D. McLean, A. Urruticoechea-Uriguen, J. R. Black, C. Elcombe, J. A. Ross, R. Wolf, W. Cui, Efficient differentiation of hepatocytes from human embryonic stem cells exhibiting markers recapitulating liver development in vivo. *Stem Cells* **26**, 894-902 (2008).
14. M. Kajiwara, T. Aoi, K. Okita, R. Takahashi, H. Inoue, N. Takayama, H. Endo, K. Eto, J. Toguchida, S. Uemoto, S. Yamanaka, Donor-dependent variations in hepatic differentiation from human-induced pluripotent stem cells. *Proc Natl Acad Sci U S A* **109**, 12538-12543 (2012).
15. K. Osafune, L. Caron, M. Borowiak, R. J. Martinez, C. S. Fitz-Gerald, Y. Sato, C. A. Cowan, K. R. Chien, D. A. Melton, Marked differences in differentiation propensity among human embryonic stem cell lines. *Nature biotechnology* **26**, 313-315 (2008).
16. H. Suemori, K. Yasuchika, K. Hasegawa, T. Fujioka, N. Tsuneyoshi, N. Nakatsuji, Efficient establishment of human embryonic stem cell lines and long-term maintenance with stable karyotype by enzymatic bulk passage. *Biochemical and biophysical research communications* **345**, 926-932 (2006).
17. W. Jelkmann, Regulation of erythropoietin production. *J Physiol* **589**, 1251-1258 (2011).
18. M. H. Rabinowitz, Inhibition of hypoxia-inducible factor prolyl hydroxylase domain oxygen sensors: tricking the body into mounting orchestrated survival and repair responses. *J Med Chem* **56**, 9369-9402 (2013).
19. K. Ataka, H. Maruyama, T. Neichi, J. Miyazaki, F. Gejyo, Effects of erythropoietin-gene electrotransfer in rats with adenine-induced renal failure. *American journal of nephrology* **23**, 315-323 (2003).
20. T. Jia, H. Olauson, K. Lindberg, R. Amin, K. Edvardsson, B. Lindholm, G. Andersson, A. Wernerson, Y. Sabbagh, S. Schiavi, T. E. Larsson, A novel model of adenine-induced tubulointerstitial nephropathy in mice. *BMC nephrology* **14**, 116 (2013).
21. R. N. Stender, W. J. Engler, T. M. Braun, F. C. Hankenson, Establishment of blood analyte intervals for laboratory mice and rats by use of a portable clinical analyzer. *Journal of the American Association for Laboratory Animal Science : JAALAS* **46**, 47-52 (2007).
22. S. Elliott, T. Lorenzini, S. Asher, K. Aoki, D. Brankow, L. Buck, L. Busse, D. Chang, J. Fuller, J. Grant, N. Hernday, M. Hokum, S. Hu, A. Knudten, N. Levin, R. Komorowski, F. Martin, R. Navarro, T. Osslund, G. Rogers, N. Rogers, G. Trail, J. Egrie, Enhancement of therapeutic protein in vivo activities through glycoengineering. *Nature biotechnology* **21**, 414-421 (2003).

23. A. Besarab, W. K. Bolton, J. K. Browne, J. C. Egrie, A. R. Nissenson, D. M. Okamoto, S. J. Schwab, D. A. Goodkin, The effects of normal as compared with low hematocrit values in patients with cardiac disease who are receiving hemodialysis and epoetin. *N Engl J Med* **339**, 584-590 (1998).
24. P. A. McFarlane, R. L. Pisoni, M. A. Eichleay, R. Wald, F. K. Port, D. Mendelssohn, International trends in erythropoietin use and hemoglobin levels in hemodialysis patients. *Kidney Int* **78**, 215-223 (2010).
25. S. Frede, P. Freitag, L. Geuting, R. Konietzny, J. Fandrey, Oxygen-regulated expression of the erythropoietin gene in the human renal cell line REPC. *Blood* **117**, 4905-4914 (2011).
26. T. Aboushwareb, F. Egydio, L. Straker, K. Gyabaah, A. Atala, J. J. Yoo, Erythropoietin producing cells for potential cell therapy. *World J Urol* **26**, 295-300 (2008).
27. M. A. Goldberg, G. A. Glass, J. M. Cunningham, H. F. Bunn, The regulated expression of erythropoietin by two human hepatoma cell lines. *Proc Natl Acad Sci U S A* **84**, 7972-7976 (1987).
28. C. K. Chiang, T. Tanaka, R. Inagi, T. Fujita, M. Nangaku, Indoxyl sulfate, a representative uremic toxin, suppresses erythropoietin production in a HIF-dependent manner. *Lab Invest* **91**, 1564-1571 (2011).
29. J. D. Quin, J. P. Miell, K. Smith, D. Gordon, J. Strachan, J. B. Dick, A. C. MacCuish, Effect of insulin-like growth factor-I therapy on erythropoetin concentrations in extreme insulin resistance. *Diabetologia* **37**, 439 (1994).
30. A. G. Bechensteen, S. Halvorsen, A. Skottner, Recombinant human insulin-like growth factor 1 (rh-IGF-1) stimulates erythropoiesis in adult, but not in newborn mice. *Acta physiologica Scandinavica* **151**, 117-123 (1994).
31. M. Sohmiya, Y. Kato, Human growth hormone and insulin-like growth factor-I inhibit erythropoietin secretion from the kidneys of adult rats. *J Endocrinol* **184**, 199-207 (2005).
32. E. D. Zanjani, J. L. Ascensao, P. B. McGlave, M. Banisadre, R. C. Ash, Studies on the liver to kidney switch of erythropoietin production. *J Clin Invest* **67**, 1183-1188 (1981).
33. W. Fried, The liver as a source of extrarenal erythropoietin production. *Blood* **40**, 671-677 (1972).
34. N. Suzuki, Erythropoietin gene expression: developmental-stage specificity, cell-type specificity, and hypoxia inducibility. *Tohoku J Exp Med* **235**, 233-240 (2015).
35. N. Asada, M. Takase, J. Nakamura, A. Oguchi, M. Asada, N. Suzuki, K. Yamamura, N. Nagoshi, S. Shibata, T. N. Rao, H. J. Fehling, A. Fukatsu, N. Minegishi, T. Kita, T. Kimura, H. Okano, M. Yamamoto, M. Yanagita, Dysfunction of fibroblasts of extrarenal origin underlies renal fibrosis and renal anemia in mice. *J Clin Invest* **121**, 3981-3990 (2011).

36. C. Befani, I. Mylonis, I. M. Gkotinakou, P. Georgoulias, C. J. Hu, G. Simos, P. Liakos, Cobalt stimulates HIF-1-dependent but inhibits HIF-2-dependent gene expression in liver cancer cells. *Int J Biochem Cell Biol* **45**, 2359-2368 (2013).
37. G. Hoppe, S. Yoon, B. Gopalan, A. R. Savage, R. Brown, K. Case, A. Vasanji, E. R. Chan, R. B. Silver, J. E. Sears, Comparative systems pharmacology of HIF stabilization in the prevention of retinopathy of prematurity. *Proc Natl Acad Sci U S A* **113**, E2516-2525 (2016).
38. J. K. Murray, C. Balan, A. M. Allgeier, A. Kasparian, V. Viswanadhan, C. Wilde, J. R. Allen, S. C. Yoder, G. Biddlecome, R. W. Hungate, L. P. Miranda, Dipeptidyl-quinolone derivatives inhibit hypoxia inducible factor-1alpha prolyl hydroxylases-1, -2, and -3 with altered selectivity. *J Comb Chem* **12**, 676-686 (2010).
39. C. E. Forristal, J. P. Levesque, Targeting the hypoxia-sensing pathway in clinical hematology. *Stem Cells Transl Med* **3**, 135-140 (2014).
40. C. M. Wyatt, T. B. Drueke, HIF stabilization by prolyl hydroxylase inhibitors for the treatment of anemia in chronic kidney disease. *Kidney Int* **90**, 923-925 (2016).
41. S. Mae, A. Shono, F. Shiota, T. Yasuno, M. Kajiwara, N. Gotoda-Nishimura, S. Arai, A. Sato-Otubo, T. Toyoda, K. Takahashi, N. Nakayama, C. A. Cowan, T. Aoi, S. Ogawa, A. P. McMahon, S. Yamanaka, K. Osafune, Monitoring and robust induction of nephrogenic intermediate mesoderm from human pluripotent stem cells. *Nat Commun* **4**, 1367 (2013).
42. Y. Taniyama, H. Hitomi, A. Shah, R. W. Alexander, K. K. Griendling, Mechanisms of reactive oxygen species-dependent downregulation of insulin receptor substrate-1 by angiotensin II. *Arterioscler Thromb Vasc Biol* **25**, 1142-1147 (2005).
43. Y. C. Wang, M. Nakagawa, I. Garitaonandia, I. Slavin, G. Altun, R. M. Lacharite, K. L. Nazor, H. T. Tran, C. L. Lynch, T. R. Leonardo, Y. Liu, S. E. Peterson, L. C. Laurent, S. Yamanaka, J. F. Loring, Specific lectin biomarkers for isolation of human pluripotent stem cells identified through array-based glycomic analysis. *Cell Res* **21**, 1551-1563 (2011).
44. K. Umeda, T. Heike, M. Nakata-Hizume, A. Niwa, M. Arai, G. Shinoda, F. Ma, H. Suemori, H. Y. Luo, D. H. Chui, R. Torii, M. Shibuya, N. Nakatsuji, T. Nakahata, Sequential analysis of alpha- and beta-globin gene expression during erythropoietic differentiation from primate embryonic stem cells. *Stem Cells* **24**, 2627-2636 (2006).

Acknowledgments

We thank Taro Toyoda, Akira Watanabe and Masaya Nagao for helpful suggestions, Tomomi Sudo, Hiromi Tanaka, Yoshiko Fujita and Md Abu Sufiun for their excellent technical assistance, and Peter Karagiannis for reading the manuscript. Pathological analysis was done by Center of Anatomical, Pathological and Forensic Medical Research, Graduate School of Medicine, Kyoto University.

Funding: This work was supported by Japan Agency for Medical Research and Development (AMED) through its research grant "Core Center for iPS Cell Research, Research Center Network for Realization of Regenerative Medicine", by a grant-in-aid for scientific research from the Ministry of Education, Culture, Sports, Science and Technology of Japan (#22790786, #22790792, #24591204 and #15K09266), by iPS Cell Research Fund, by Sanju Alumni Research Grant, by Kanae Foundation for the Promotion of Medical Science and by Daiichi Sankyo Foundation of Life Science.

Author contributions: H.H., A.N., and K.O. conceived the project. H.H., A.N., and K.O. designed the experiments. H.H., T.K., N.K., A.H., S.M, M.K., T.T., A.R., D.N., A.N., M.K.S., T.N., A.N., and K.O. performed the experiments. H.H., S.M, A.N., M.K.S., T.N., A.N., and K.O. analyzed the data. H.H., A.N., M.K.S., T.N., A.N., and K.O. wrote the manuscript.

Competing interests: H.H. and K.O. holds a patent entitled "Method for inducing erythropoietin-producing cell" on US61/621,256, PCT/JP2013/060878, JP2014-509231, US14/390853, US9334475, EP13773017.2.

Figures legends

Fig. 1. Differentiation of hiPSCs/ESCs into EPO-producing cells.

(**A**) The expression of *EPO* mRNA was examined in human fetal and adult liver tissue, human fetal and adult kidney and human adult brain tissue. Bacterial artificial chromosome (BAC) containing *EPO* cDNA was used as a positive control. (**B**) EPO protein expression was evaluated using immunocytochemistry. Fetal mouse liver (E12.5) was positively stained with anti-EPO (green) and anti-AFP (red) antibodies. (**C**) The expression of marker genes for endoderm and liver lineages and *EPO* in cultures of differentiated hiPSCs. Human liver specimens were used as a positive control. hiPSCs were differentiated into hepatic lineage (Stage 1 to 3) as shown in Figure S1. (**D, E**) Time-course analyses of the expression of *EPO* mRNA (**D**) and protein (**E**). The expression of *EPO* mRNA was measured using qRT-PCR in (**D**), and Western blotting was performed with anti-EPO antibodies in (**E**). Each value was normalized to that of the samples on day 0 before treatment with Stage 2 medium. (**F**) EPO protein expression was evaluated using immunocytochemistry. hiPSC-EPO cells were positively stained with anti-EPO (green) and anti-AFP (red) antibodies. (**G**) Secretory vesicles (black arrows) were observed in the cytoplasm of hiPSC-EPO cells by transmission electron microscopy. The right lower panel is an image of E11.5 fetal mouse liver for comparison. (**H**) A temporal analysis of the EPO protein concentrations in the culture media of hiPSC-EPO cells measured using ELISA. (**I**) *EPO* mRNA expression was observed in the differentiation cultures of multiple hiPSC/ESC lines. Each value was normalized to that of the samples on day 0 before treatment with Stage 2 medium in a hiPSC line, 253G4. The data were obtained from four independent experiments and are presented as the mean ± SEM in (**D**), (**E**), (**H**) and (**I**). *$p < 0.05$ vs. day 0 in (**D**), (**E**) and (**H**); analysis of variance (ANOVA) with Bonferroni's test. Scale bars, 40 μm in (**B, F**) and 2 μm in (**G**).

Fig. 2. Cell proliferation and EPO-producing capacity of hiPSC-EPO cells.

(**A**) The number of hiPSC-EPO cells at Stage 2. hiPSCs were differentiated into EPO-producing cells (Stage 2) as shown in Figure S1. (**B**) The expression of a cell proliferation marker, Ki67, was measured by immunocytochemistry. (**C**) The number of hiPSC-EPO cells cultured using *in vitro* maintenance culture method. (**D, E**) Time-course analyses of *EPO* mRNA expression (**D**) and EPO protein secretion (**E**) by RT-PCR and EPO ELISA, respectively. Each value was normalized to that of the samples on Stage 2 day 0 in (**D**). The data from four independent experiments are presented as the mean ± SEM in (**A**), (**C**), (**D**) and (**E**). *$p < 0.05$ vs. day 0 in (**A**), (**D**) and (**E**); analysis of variance (ANOVA) with Bonferroni's test. Scale bars, 40 μm in (**B**).

Fig. 3. Differentiation of EPO-producing cells from mouse iPSCs/ESCs.

(A) The temporal pattern of mouse *Epo* mRNA expression in the differentiation culture of a miPSC line, 494B-4, measured using qRT-PCR. Each value was normalized to that of the samples on day 0 before treatment with Stage 2 medium. (**B**) *Epo* mRNA expression was observed in the differentiation culture of a mESC line, D3. Each value was normalized to that of the samples on day 0 before treatment at Stage 2 in the 494B-4 miPSC line. (**C**) The mouse EPO protein concentrations in the cell culture media of Stage 2 cells were measured using ELISA. The data were obtained from four independent experiments and are presented as the mean ± SEM. *$p < 0.05$ vs. day 0; Student's *t*-tests (**B**) and analysis of variance (ANOVA) with Bonferroni's test (**C**).

Fig. 4. Effects of IGF-1 treatment on EPO expression and secretion in hiPSC-EPO cells.

(A) Effects of IGF-1, IGF-2 and insulin treatment on the *EPO* mRNA expression at Stage 2 culture day 8 of hiPSC-EPO cells using qRT-PCR analysis. Each value was normalized to that of control samples (no growth factor). A sample of human fetal liver was used as a positive control. (**B**) IGF-1 receptor expression was measured using Western blot analysis. Representative data are shown for four independent experiments. (**C, D**) Concentration-dependent effects of IGF-1 treatment on EPO mRNA expression (**C**) and protein secretion (**D**) in Stage 2 day 8 of hiPSC-EPO cells. Each value was normalized to that of control hiPSCs treated with no IGF-1. (**E, F**) Time-course analyses of the IGF-1-induced *EPO* mRNA expression (**E**) and protein secretion (**F**) in hiPSC-EPO cells. Each value was normalized to that of samples on day 0 before treatment with Stage 2 medium in (**E**). (**G, H**) The mRNA expression of *AFP* (**G**) and *ALBUMIN* (**H**) was analyzed using qRT-PCR. Each value was normalized to control hiPSC-EPO cells treated with no IGF-1 on Stage 2 day 8. The data were obtained from four independent experiments and are presented as the mean ± SEM in (**A**) and (**C**) – (**H**). *$p < 0.05$ vs. control samples without IGF-1 treatment in (**A**) and (**C**) – (**F**); analysis of variance (ANOVA) with Bonferroni's test.

Fig. 5. Stimulation of EPO expression and secretion under hypoxic culture conditions.

(**A, B**) Time-course analyses of *EPO* mRNA expression (**A**) and protein secretion (**B**) in hiPSC-EPO cells cultured under low oxygen (1%) conditions compared to control hiPSC-EPO cells cultured under normal oxygen (21%) conditions. *EPO* mRNA expression was measured using qRT-PCR, whereas the EPO protein concentrations in the culture media were analyzed using ELISA. Each value was normalized to that of samples on day 0 before treatment with Stage 2

medium in (**A**). (**C, D**) *AFP* (**C**) and *ALBUMIN* (**D**) mRNA expression was analyzed using qRT-PCR. Each value was normalized to hiPSC-EPO control samples under normoxic conditions on Stage 2 day 8. **(E, F**) The effects of PHD inhibitors on *EPO* mRNA expression (**E**) and protein secretion (**F**) in hiPSC-EPO cells on Stage 2 day 8 and HepG2 cells were analyzed using qRT-PCR and ELISA, respectively. deferoxamine 100 μM, FG4592 50 μM, DMOG 1 mM. Each value was normalized to control samples (no PHD inhibitor) in (**E**). **(G**) The effects of a HIF-1 dimerization inhibitor, Acriflavine (10 μM), on EPO protein secretion in hiPSC-EPO cells. (**H**) The nuclear translocation of HIF-1α and HIF-2α in hiPSC-EPO cells and HepG2 cells under hypoxic (1%) conditions was evaluated by immunocytochemistry. The data from four independent experiments are presented as the mean ± SEM. *$p < 0.05$ vs. control samples under normoxic conditions in (**A**) and (**B**) or without factors in (**E**) – (**G**). **$p < 0.05$ vs. control samples (HepG2 cells) in (**E**) and (**F**); analysis of variance (ANOVA) with Bonferroni's test (**A**), (**B**), (**E**) and (**F**) and Student's *t*-tests (**G**). Scale bars, 20 μm in (**H**).

Fig. 6. Effects of hiPSC-EPO protein on erythropoiesis *in vitro*.

(**A**) Schematic of clonogenic hematopoietic progenitor assays using methylcellulose-based semi-solid medium. (**B**) Representative images of BFU-E (erythroid burst-forming unit) induced by human recombinant EPO (rhEPO) (left) and hiPSC-EPO protein (right). (**C**) The number of clonal colonies on semi-solid medium containing stem cell factor, thrombopoietin and interleukin 3 (ST3) supplemented with 0.28 and 2.8 ng/mL of rhEPO or hiPSC-EPO protein (n = 3). (**D**) The number of clonal colonies on semi-solid medium containing different concentrations of neutralizing antibodies against human EPO in addition to ST3 and 2.8 ng/mL of hiPSC-EPO protein (n = 3).

The data were obtained from three independent experiments and are presented as the mean ± SEM in (**C**) and (**D**). CFU-GM: granulocyte–macrophage colony-forming units, CFU-Mix: mixed colony-forming units. Scale bars, 200 μm in (**B**).

Fig. 7. Therapeutic effects of hiPSC-EPO protein on renal anemia in adenine-treated mice.

(**A** - **H**) Renal anemia was induced using adenine treatment (50 mg/kg body weight daily for 4 weeks) in male C57BL/6 mice. The mice were then treated with recombinant human EPO (rhEPO) or hiPSC-EPO protein. (**A**) Time-course analyses of the hematocrit measured using glass capillary tubes. (**B**) Hematocrit after four weeks of treatment with rhEPO or hiPSC-EPO protein. (**C**) Hemoglobin concentrations after four weeks of treatment analyzed using ELISA. The gray shaded areas indicate the normal hematocrit in C57BL/6 mice in (**A**) and (**B**) and that of Hb concentrations in C57BL/6 mice in (**C**). (**D**) The number of red blood cells (RBC), white blood cells (WBC) and platelets after four weeks of treatment. (**E**) The mean corpuscular volume (MCV), mean corpuscular hemoglobin (MCH) and mean corpuscular hemoglobin concentration (MCHC) after four weeks of treatment. (**F, G**) The concentrations of mouse (**F**) and human (**G**) EPO protein in mouse serum were measured after four weeks of treatment using ELISA. (**H**) The efficiency of renal anemia recovery following treatment with 0.56 ng of rhEPO or hiPSC-EPO protein was calculated based on the increase in hematocrit per week (ΔHct/week). (**I**) Glycosylation patterns of hiPSC-EPO and rhEPO protein were measured by lectin microarray assay. The data are presented as the mean ± SEM (n = 4). Abbreviations are defined in Supplementary Table S3. (**J**) Half-lives of the hiPSC-EPO and rhEPO proteins *in vivo* were evaluated by measuring EPO protein concentrations in mouse serum after subcutaneous injection of hiPSC-EPO or rhEPO protein using

ELISA. The data from three independent experiments are presented as the mean ± SEM in (**A**) – (**H**) and (**J**). n = 6 for control and n = 10 for rhEPO 28 ng, rhEPO 0.56 ng, hiPSC-EPO protein 0.56 ng and saline. *p < 0.05 vs. saline in (**A**) – (**D**), control in (**G**) and rhEPO in (**H**); analysis of variance (ANOVA) with Bonferroni's test (**A**) – (**G**) and Student's *t*-tests (**H**).

Fig. 8. Therapeutic effects of the transplantation of hiPSC-EPO-producing cells on renal anemia in adenine-treated mice.

Renal anemia was induced using adenine treatment (50 mg/kg body weight daily for 5 weeks) in immunodeficient mice (NOD.CB17-*Prkdc*^{scid}/J mice). Twenty aggregates of hiPSC-EPO-producing cells (5.0×10^5 cells/aggregate) were transplanted into the kidney subcapsules of mice with renal anemia. (**A**) Hematocrit was examined during the first four weeks after transplantation using glass capillary tubes. (**B**) Human EPO concentrations in mouse serum at four weeks after transplantation were measured using ELISA. (**C**) Hematocrit was examined for up to 28 weeks after transplantation. The gray shaded areas in (**A**) and (**C**) indicate the normal hematocrit range in NOD.CB17-*Prkdc*^{scid}/J mice. (**D**) Human EPO concentrations in mouse serum after transplantation were measured using ELISA. (**E**) The hiPSC-EPO-producing cell grafts were evaluated using immunohistochemistry for EPO (green), AFP (red) and ALBUMIN (red), and Hematoxylin and eosin (H&E) staining. (**F**) The new vasculature in the grafts derived from host mice was examined by anti-mouse CD31/PECAM-1 immunostaining and H&E staining. (**G**) The human EPO concentrations in host mouse serum after phlebotomy were measured using ELISA. The data from three independent experiments are presented as the mean ± SEM, n = 6 for hiPSC-EPO-producing cells and saline in (**A**) and (**B**). The data from two independent experiments are

presented as the mean ± SEM, n = 4 for hiPSC-EPO cells and saline in (**C**), (**D**) and (**G**). *p < 0.05 vs. control; analysis of variance (ANOVA) with Bonferroni's test (**A**), (**C**), (**D**) and (**G**) and Student's *t*-tests (**B**). Scale bars, 40 μm in (**E**) and 20 μm in (**F**).

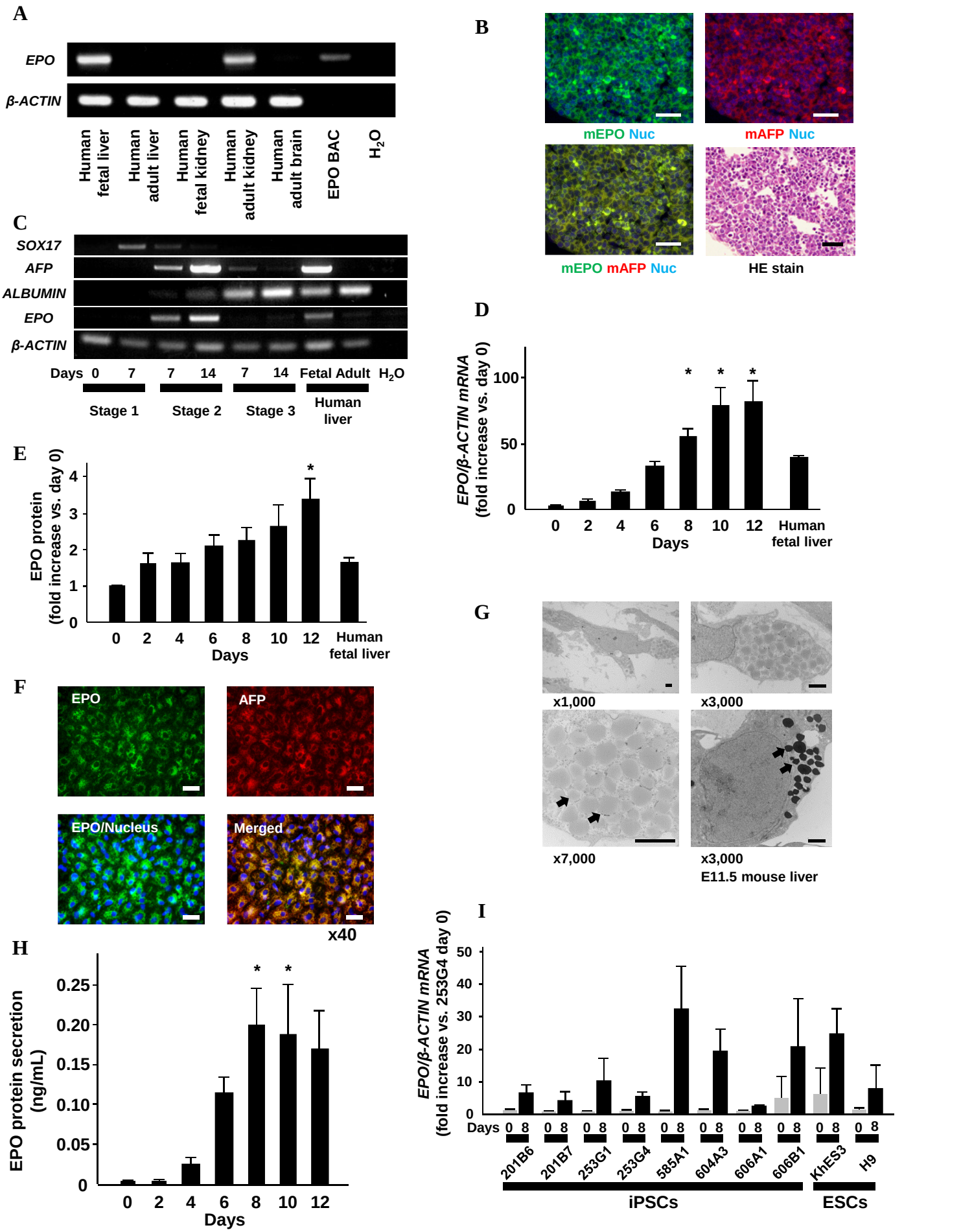

Fig. 1. Differentiation of hiPSCs/ESCs into EPO-producing cells.

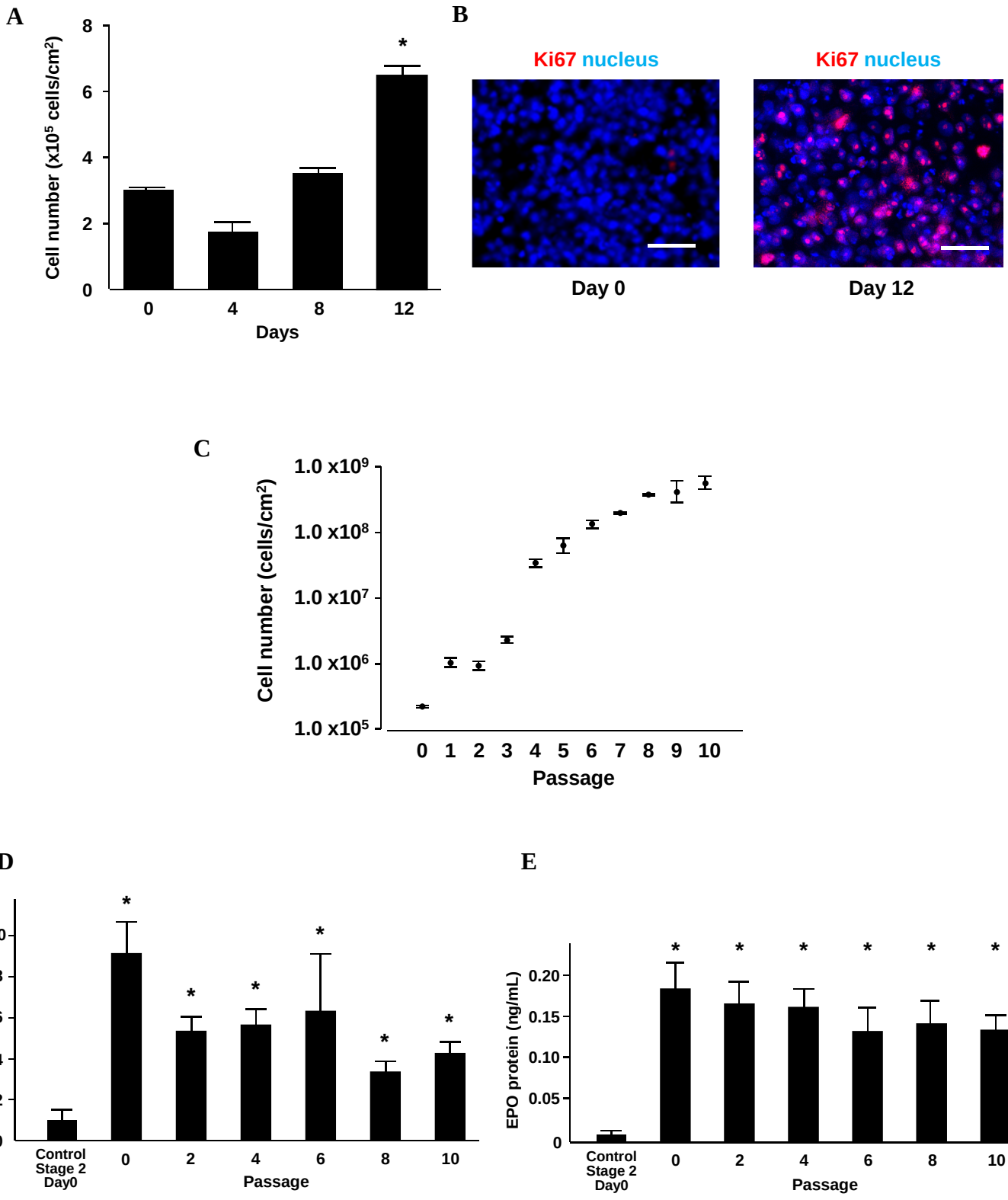

Fig. 2. Cell proliferation and EPO-producing capacity of hiPSC-EPO cells.

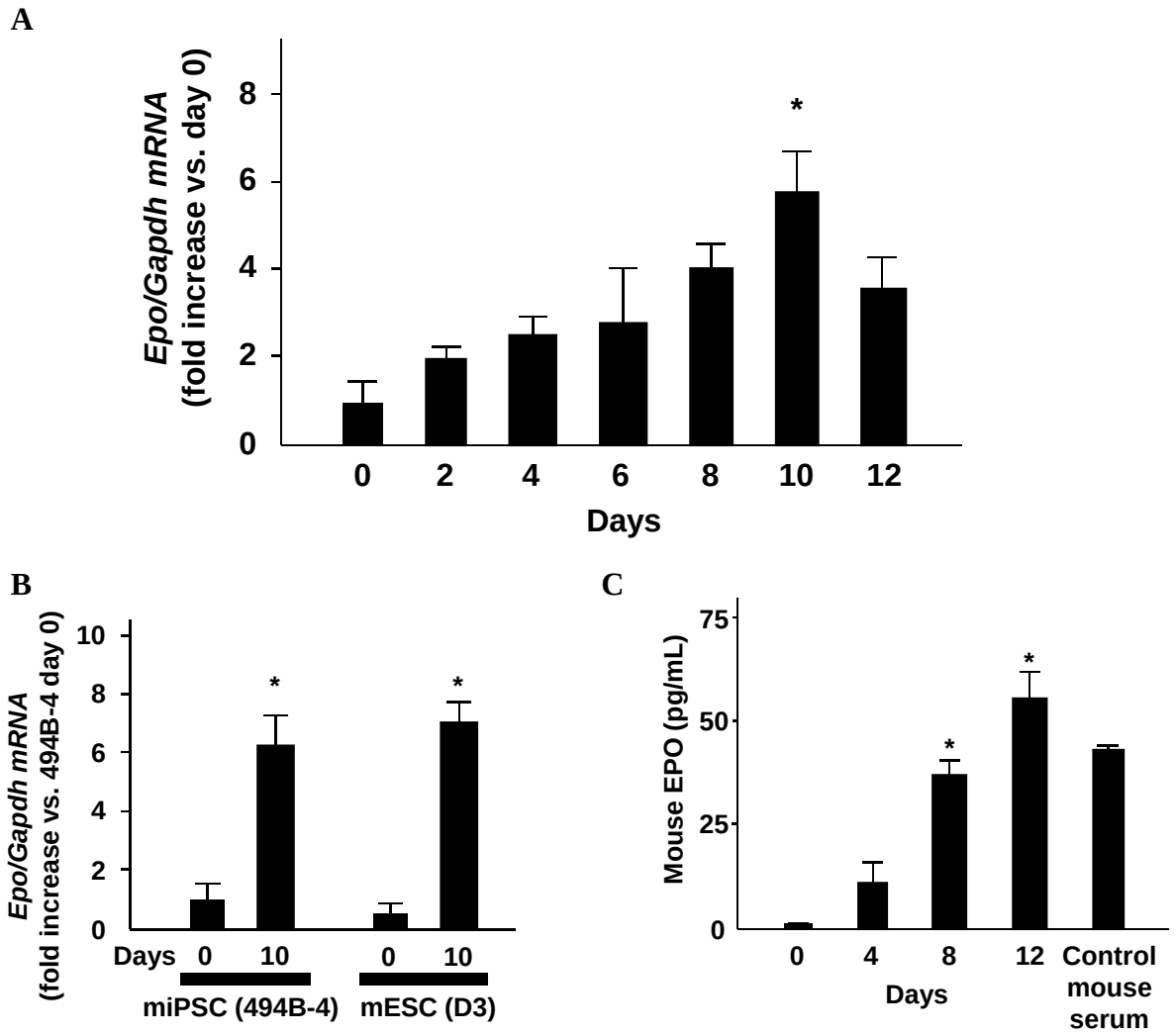

Fig. 3. Differentiation of EPO-producing cells from mouse iPSCs/ESCs.

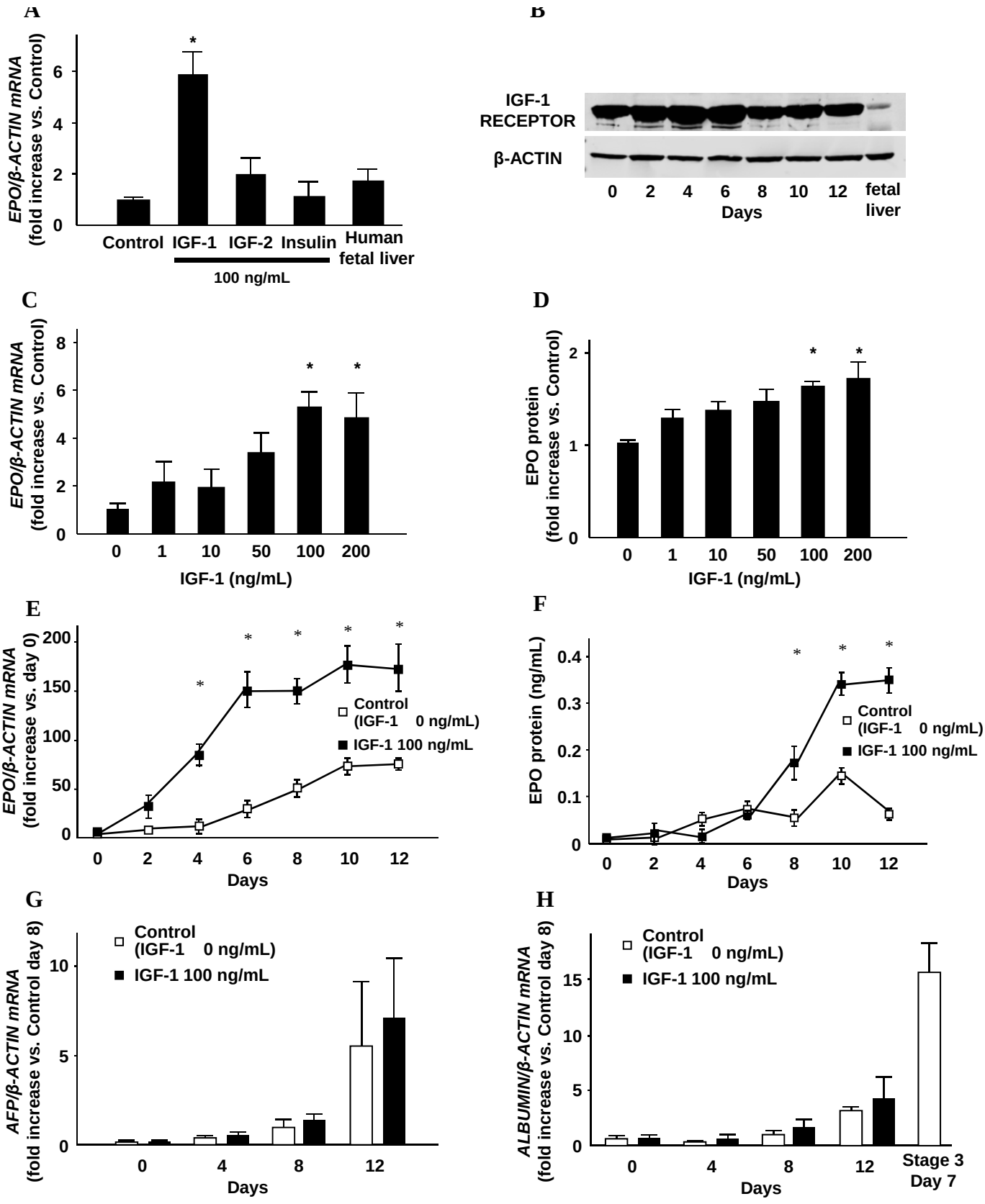

Fig. 4. Effects of IGF-1 treatment on EPO expression and secretion in hiPSC-EPO cells.

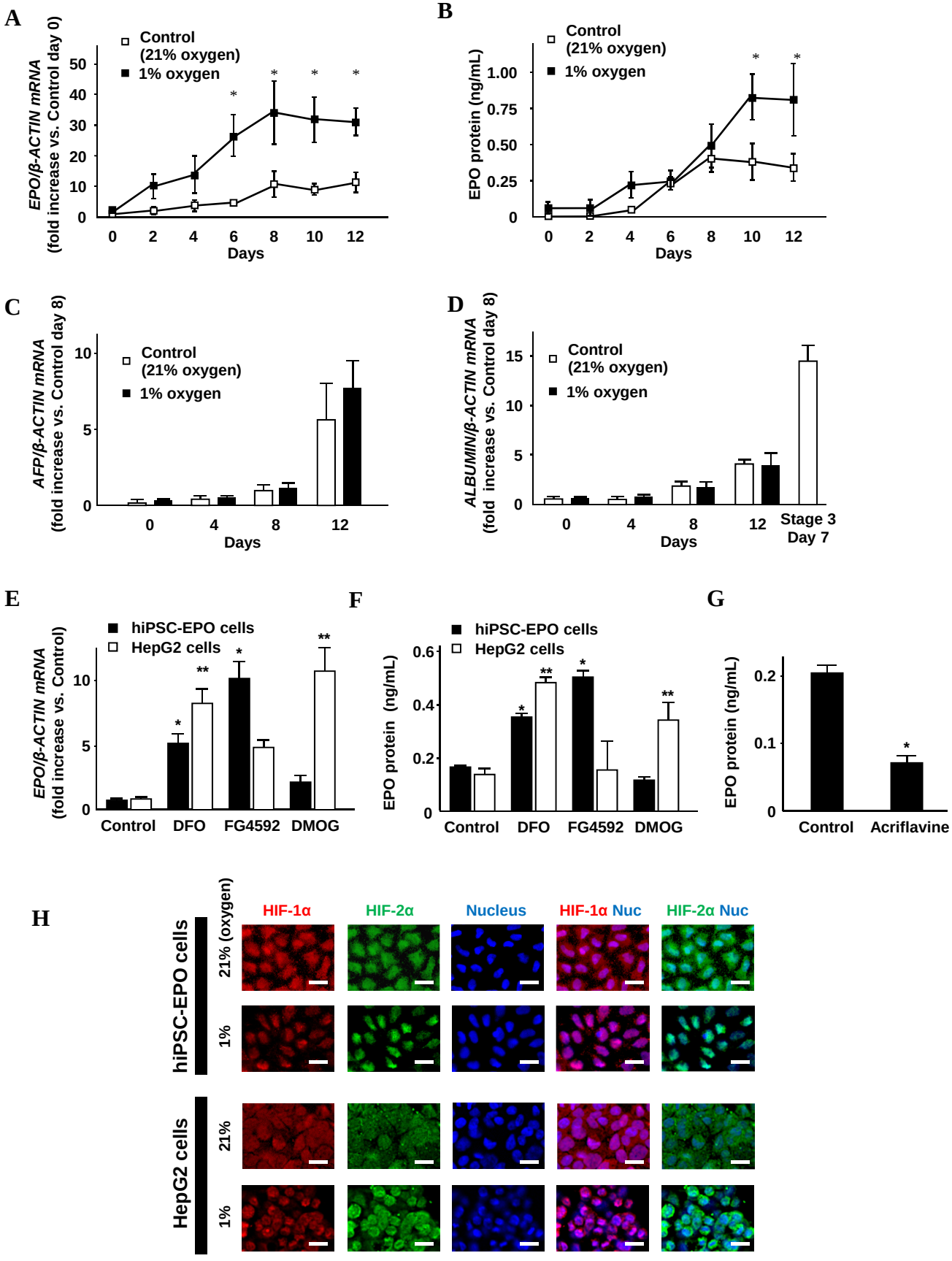

Fig. 5. Stimulation of EPO expression and secretion under hypoxic culture conditions.

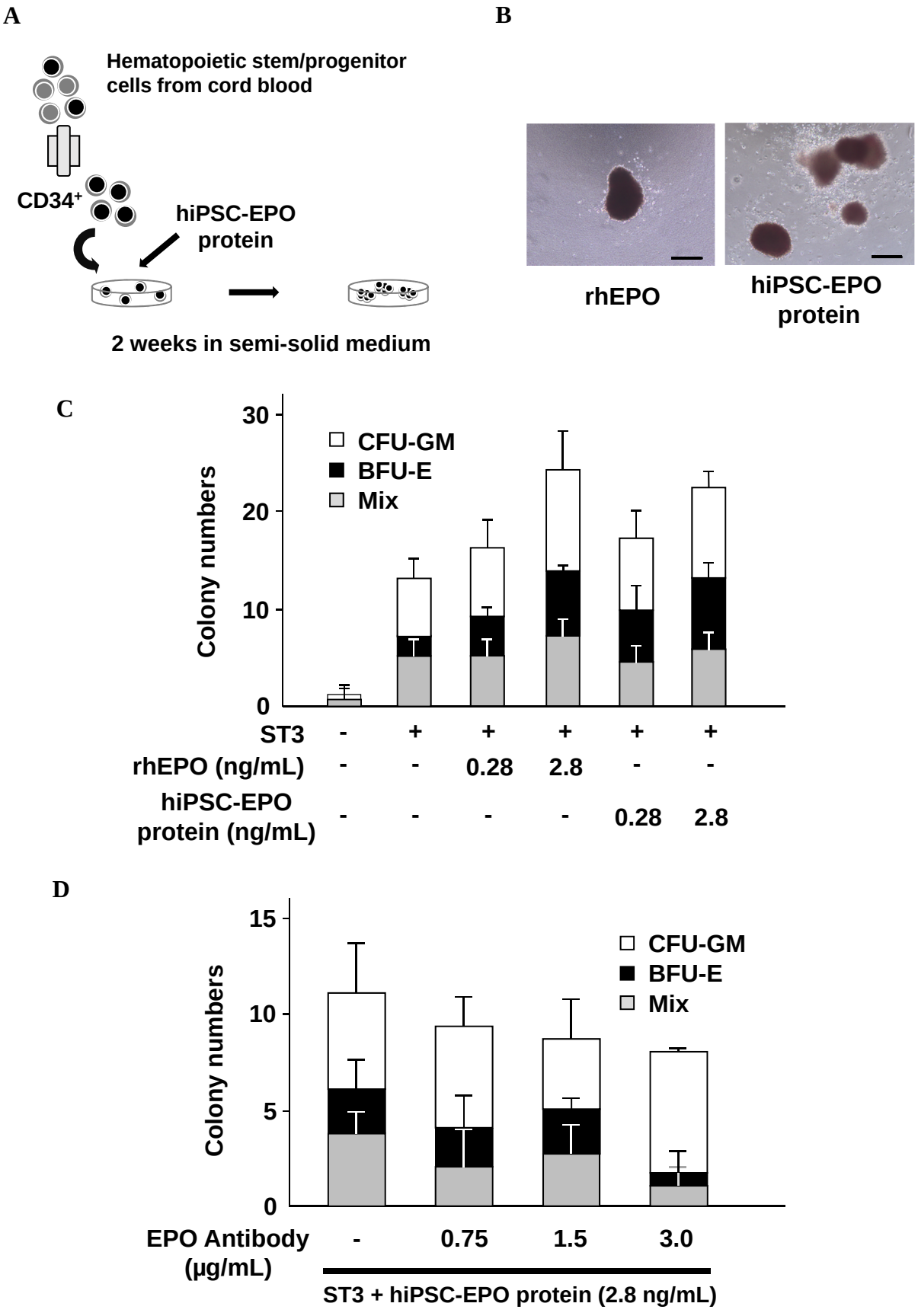

Fig. 6. Effects of hiPSC-EPO protein on erythropoiesis in vitro.

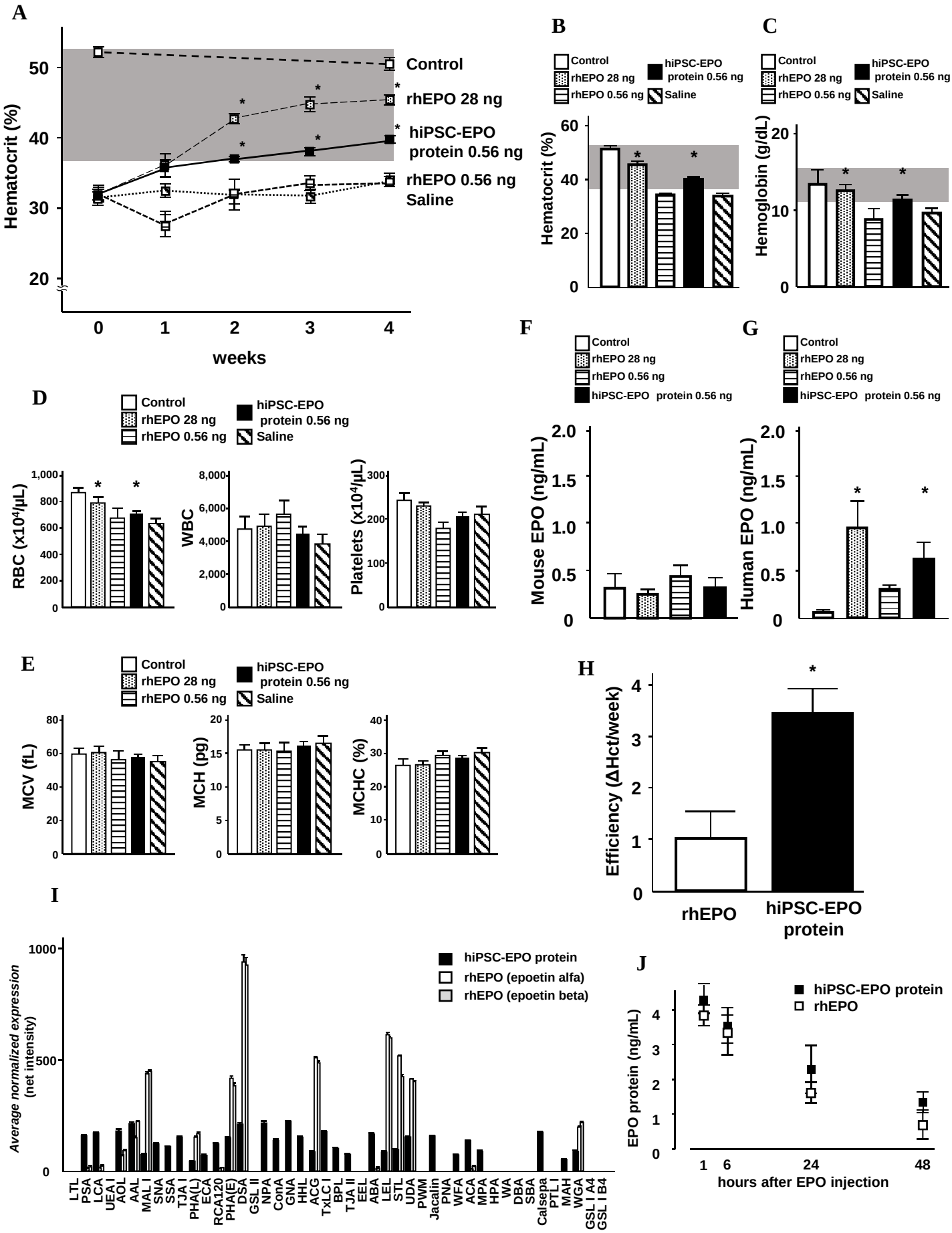

Fig. 7. Therapeutic effects of hiPSC-EPO protein on renal anemia in adenine-treated mice.

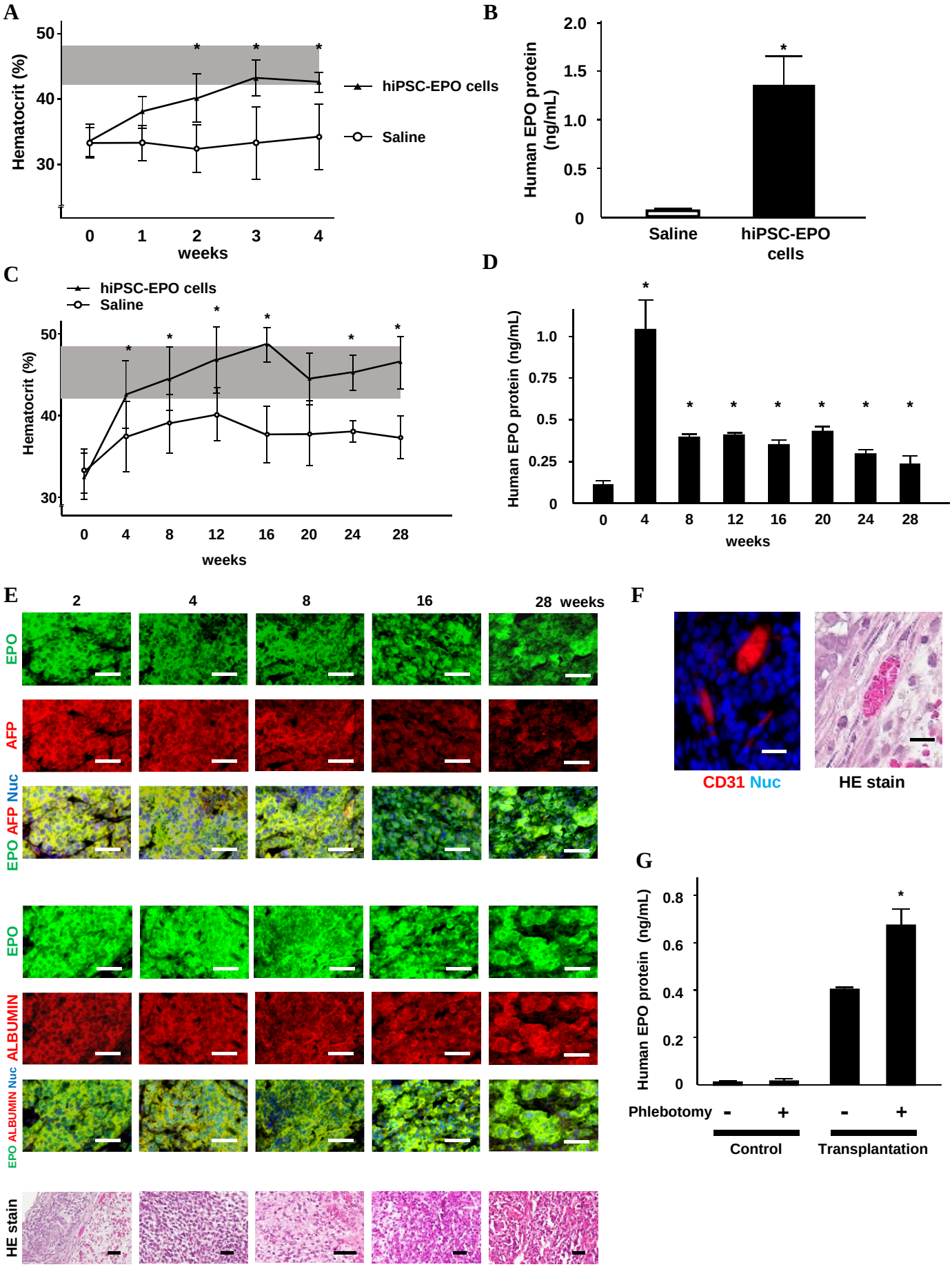

Fig. 8. Therapeutic effects of the transplantation of hiPSC-EPO-producing cells on renal anemia in adenine-treated mice.

Supplementary Materials for

Human pluripotent stem cell-derived erythropoietin-producing cells improve renal anemia in mice

Hirofumi Hitomi[1,2], Tomoko Kasahara[1], Naoko Katagiri[1], Azusa Hoshina[1], Shin–Ichi Mae[1], Maki Kotaka[1], Takafumi Toyohara[1], Asadur Rahman[2], Daisuke Nakano[2], Akira Niwa[3], Megumu K. Saito[3], Tatsutoshi Nakahata[3], Akira Nishiyama[2], Kenji Osafune[1]*

[1]Department of Cell Growth and Differentiation, Center for iPS Cell Research and Application (CiRA), Kyoto University, Kyoto, Japan.
[2]Department of Pharmacology, Faculty of Medicine, Kagawa University, Kagawa, Japan.
[3]Department of Clinical Application, Center for iPS Cell Research and Application (CiRA), Kyoto University, Kyoto, Japan.

All correspondence to:
Kenji Osafune, M.D., Ph.D.
Department of Cell Growth and Differentiation, Center for iPS Cell Research and Application (CiRA), Kyoto University, Kyoto, Japan
53 Kawahara-cho, Shogoin, Sakyo-ku, Kyoto 606-8507, Japan
Tel: +81-75-366-7058
Fax: +81-75-366-7077
E-mail: osafu@cira.kyoto-u.ac.jp

Supplemental Figures

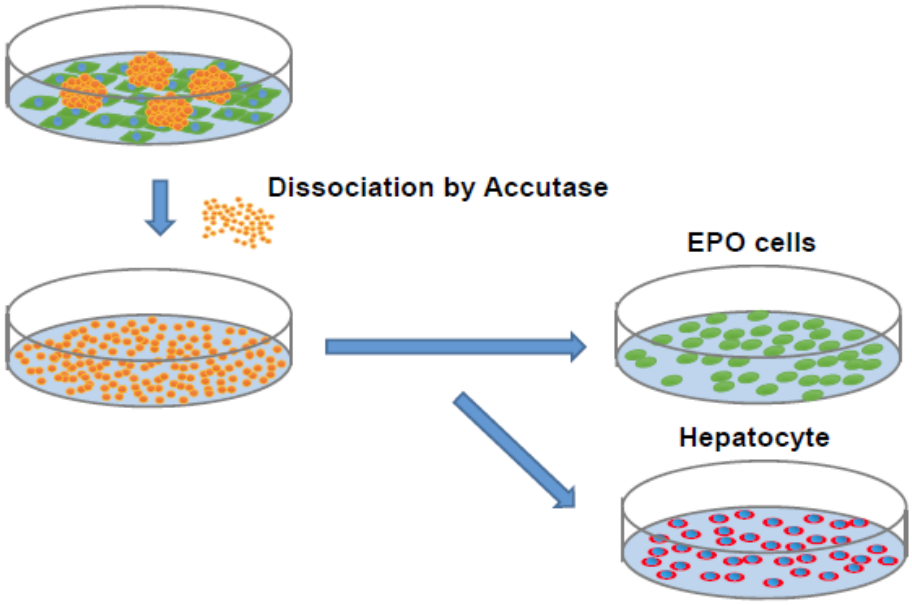

Culture days

	0	1	3	7	EPO cells
Stage	Stage 1 (7 days)				Stage 2 (14 days)
Medium	RPMI 1640				KnockOut DMEM
Factor(s)	Activin A (100 ng/mL) CHIR99021 (1 μM) Y-27632 (10 μM)	Activin A (100 ng/mL) CHIR99021 (1 μM) NaB (0.5 mM)	Activin A (100 ng/mL) CHIR99021 (1 μM)		DMSO (1%)

14	Hepatocyte	21
Stage 3 (7 days)		
Hepatocyte culture medium		
HGF (10 ng/mL) Oncostatin M (20 ng/mL)		

Fig. S1. Differentiation method for generating EPO-producing cells from hiPSCs/ESCs.

The differentiation of EPO cells from hiPSCs/ESCs was performed by modifying a previously reported protocol for hepatic lineage. Colonies of hiPSCs/ESCs grown on a SNL feeder layer were

dissociated to single cells via gentle pipetting after treatment with Accutase and seeded on Matrigel-coated plates with Stage 1 medium containing RPMI 1640 supplemented with penicillin/streptomycin, B27 supplement, recombinant human/mouse/rat activin A and CHIR99021. Y-27632 was added to Stage 1 medium for the first 24 hours. Thereafter, NaB was supplemented to Stage 1 medium until culture day 3. On day 7, the medium was changed to Stage 2 medium containing Knockout DMEM supplemented with penicillin/streptomycin, KSR, DMSO, L-glutamine, non-essential amino acid and β-mercaptoethanol. To produce EPO cells, Stage 2 treatment was kept for 14 days. For hepatocyte differentiation, the culture was shifted to the hepatocyte maturation step after 7 days of Stage 2 treatment using incubation with Stage 3 medium containing hepatocyte culture medium supplemented with HGF and Oncostatin M.

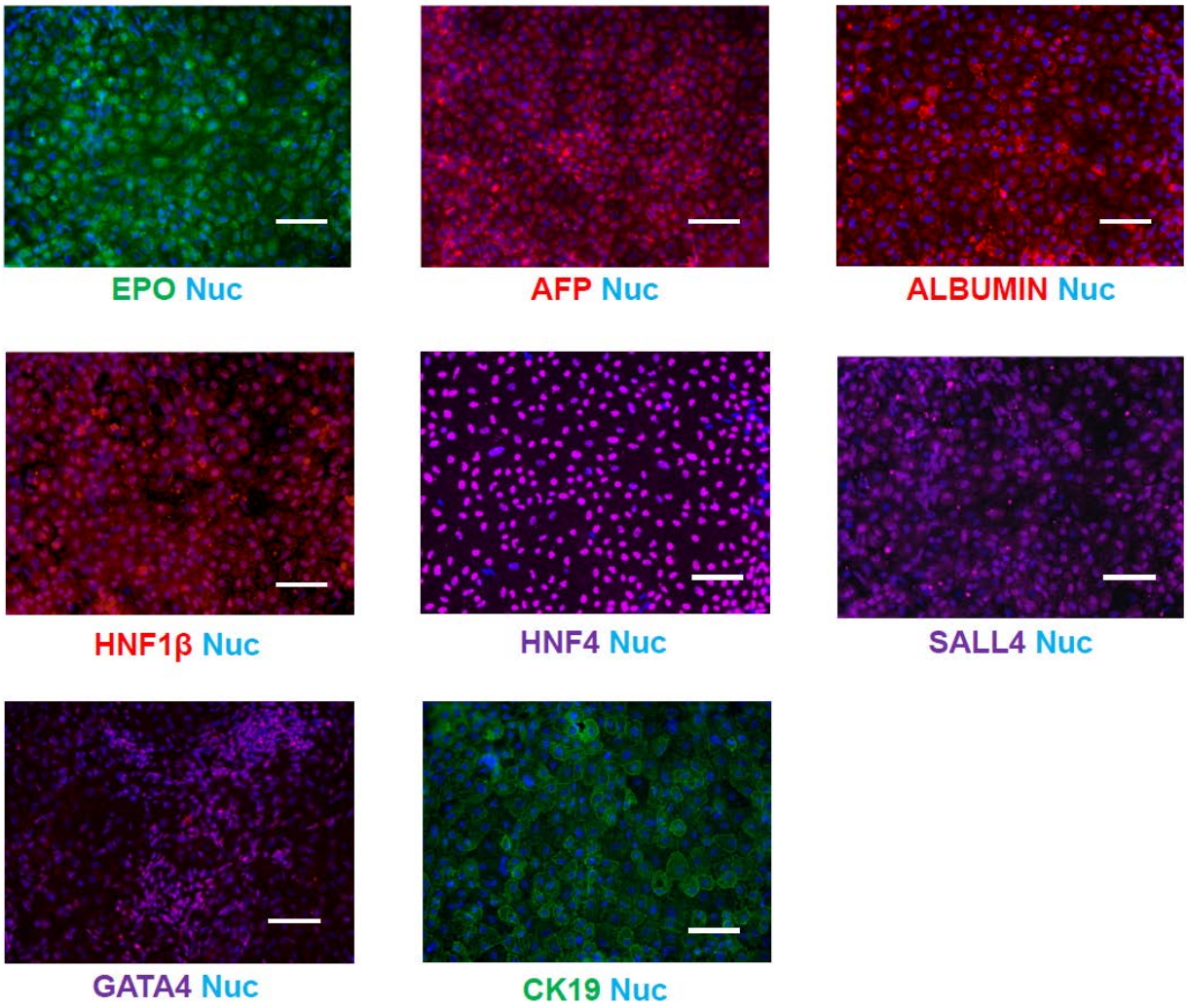

Fig. S2. Expression of hepatic lineage and endoderm markers in hiPSC-EPO cells.

Hepatic lineage markers, AFP (red) and ALBUMIN (red), and endoderm markers, HNF1β (red), HNF4 (purple), SALL4 (purple), GATA4 (purple) and CK19 (green), were measured by immunocytochemistry. Scale bars, 40 μm.

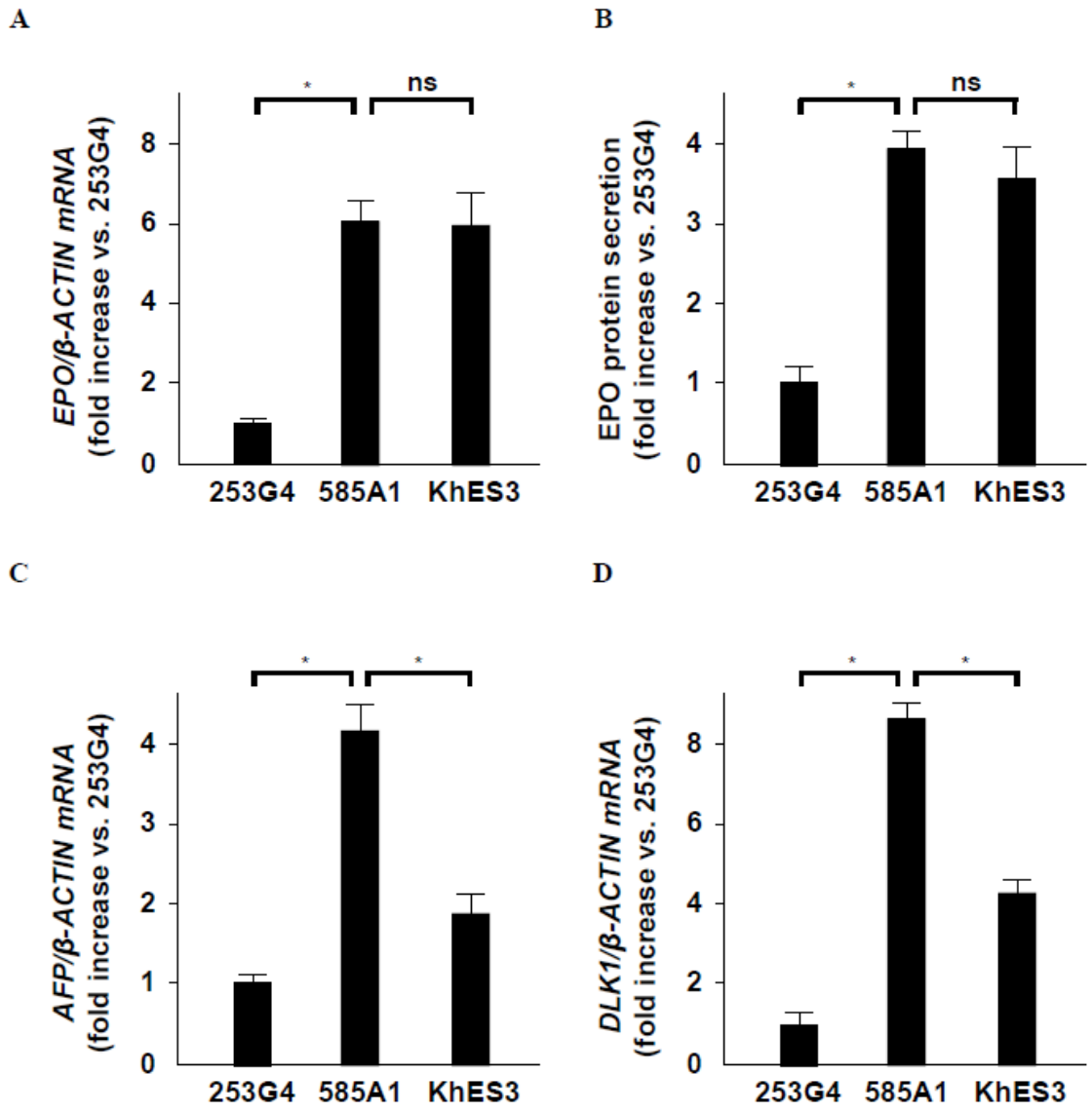

Fig. S3. Variable expression and secretion of EPO and expression of hepatoblast markers among three hiPSC/ESC lines.

EPO mRNA expression (**A**) and protein secretion (**B**) and mRNA expression of hepatoblast markers AFP (**C**) and DLK1 (**D**) were measured on Stage 2 day 8 of differentiation cultures with two hiPSC lines (253G4 and 585A1) and one hESC line (KhES3). Each value was normalized to that of the samples of 253G4. The data were obtained from four independent experiments and are presented as the mean ± SEM. *$p < 0.05$. ns: not significant; analysis of variance (ANOVA) with Bonferroni's test.

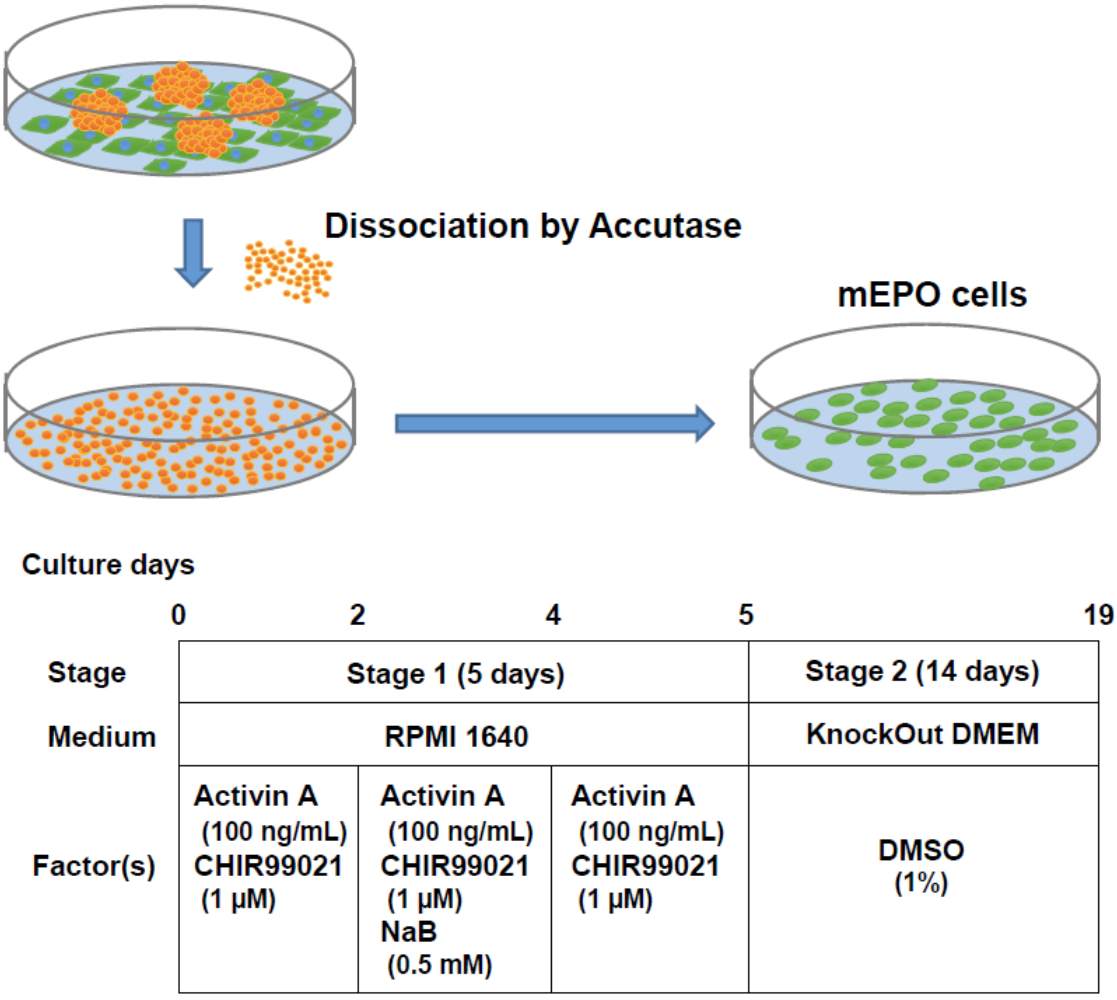

Fig. S4. Differentiation method for generating EPO-producing cells from miPSCs/ESCs.

The differentiation of EPO cells from miPSCs/ESCs was performed using a similar protocol to that for hiPSCs/ESCs. miPSCs/ESCs dissociated to single cells with Accutase treatment were cultured with Stage 1 medium containing RPMI 1640, penicillin/streptomycin, B27 supplement, activin A and CHIR99021. After two days, the medium was supplemented with NaB until culture day 4. On day 5, the medium was changed to Stage 2 medium containing Knockout DMEM supplemented with penicillin/streptomycin, KSR, DMSO, L-glutamine, non-essential amino acid and β-mercaptoethanol, and Stage 2 treatment was kept for 14 days to produce EPO cells.

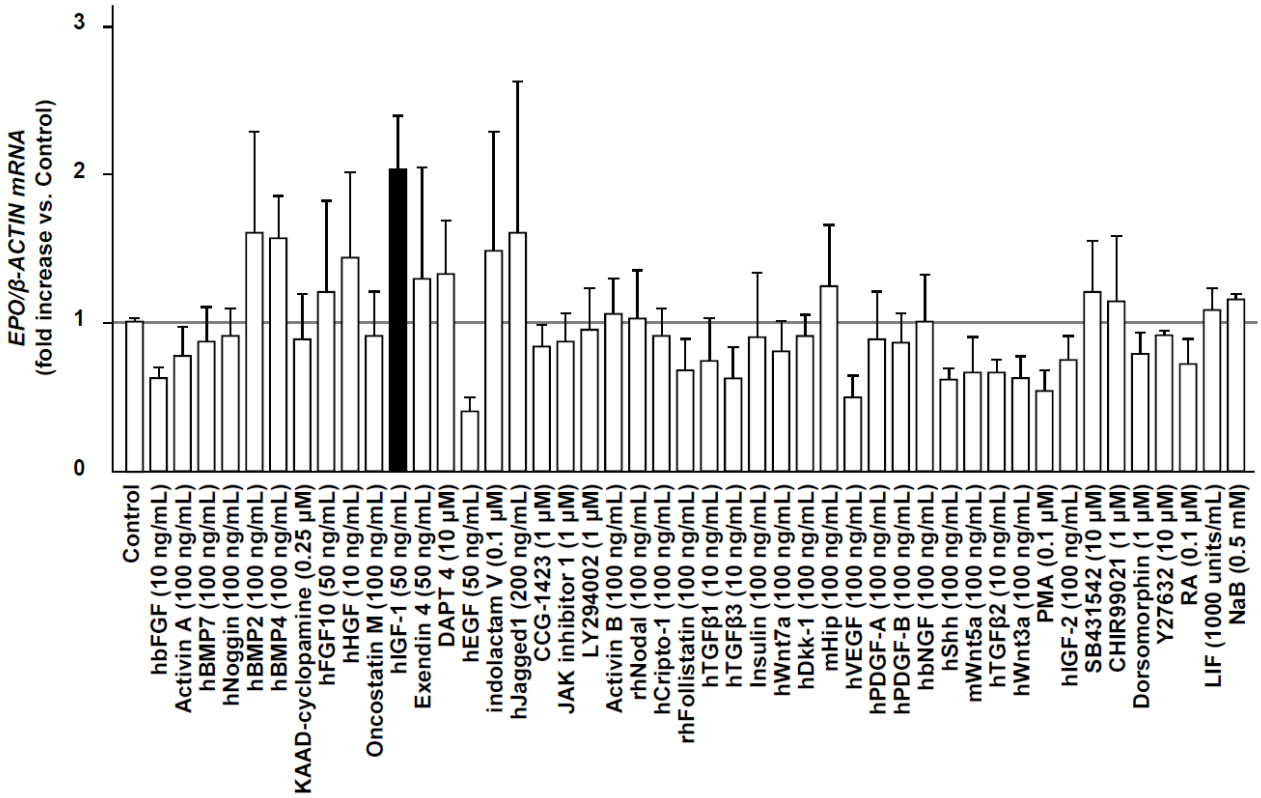

Fig. S5. Effects of 46 different factors on *EPO* mRNA expression in hiPSC-EPO cells.

The effects of 46 different factors (growth factors and chemical compounds) on *EPO* expression in hiPSC-EPO cells were measured using qRT-PCR. The data were obtained from three independent experiments and are presented as the mean ± SEM. Samples without factors were used as a control to normalize the results. The black bar indicates the sample treated with human IGF-1.

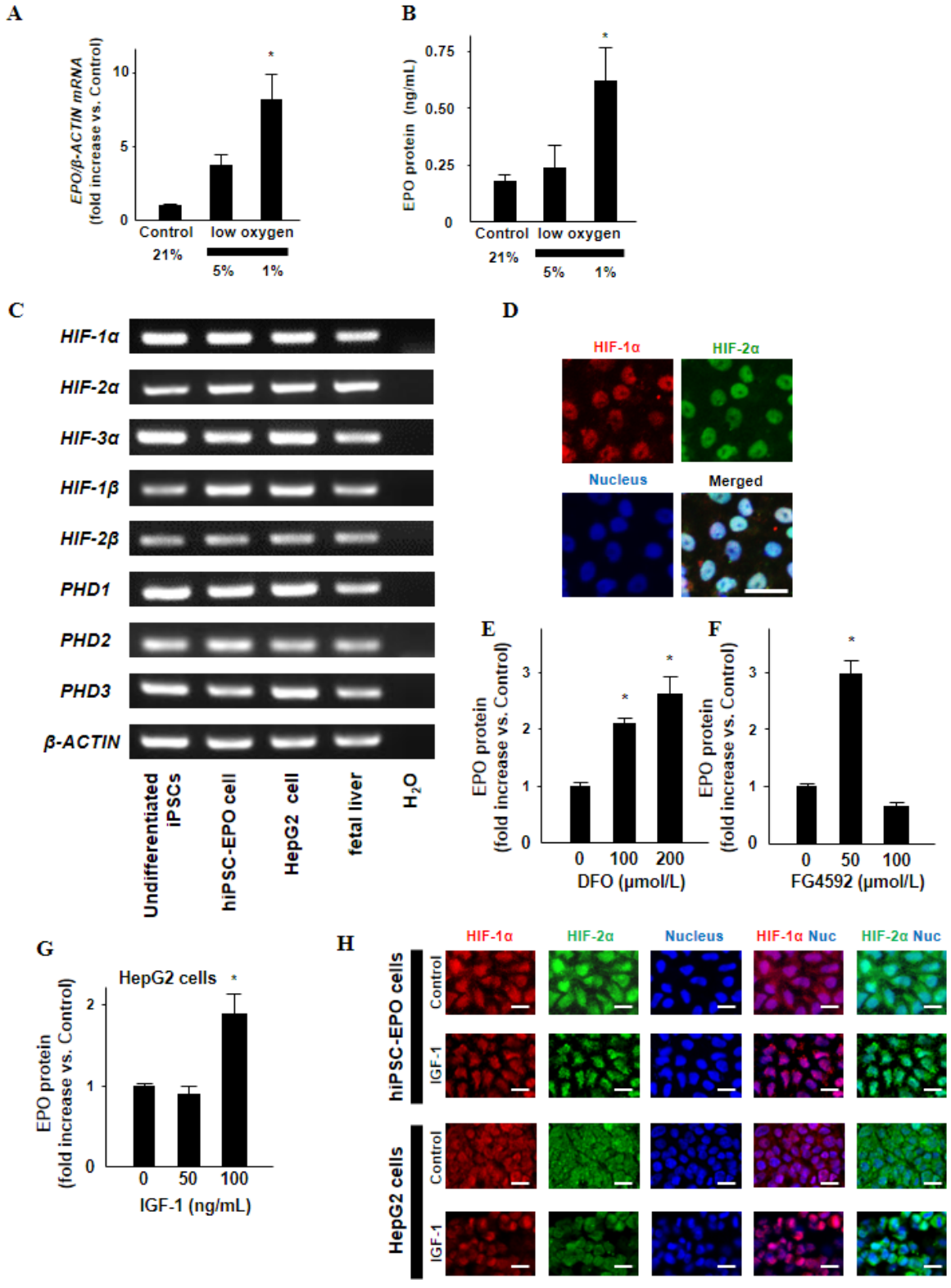

Fig. S6. The HIF-PHD pathway regulates EPO production induced by hypoxia or IGF-1 treatment.

(A, B) EPO mRNA expression (**A**) and protein secretion (**B**) in hiPSC-EPO cells cultured under three oxygen concentrations (21%, 5% and 1%) on Stage 2 day 8. The *EPO* mRNA expression was measured using qRT-PCR while the EPO protein concentration in the culture media was analyzed using ELISA. Each value was normalized to that of control (21%) in (**A**). (**C**) The expression of *HIF* and *PHD* mRNAs was examined in undifferentiated hiPSCs, hiPSC-EPO cells, HepG2 cells and human fetal liver. **(D)** HIF-1α and HIF-2α protein expression was measured by immunocytochemistry in hiPSC-EPO cells treated with FG4592. **(E, F)** EPO protein secretion induced by different doses of DFO **(E)** and FG4592 **(F)** in hiPSC-EPO cells on Stage 2 day 8 was measured by ELISA. **(G)** EPO protein secretion in HepG2 cells induced by IGF-1 treatment was measured by ELISA. (**H**) The nuclear translocation of HIF-1α and -2α in hiPSC-EPO and HepG2 cells with IGF-1 treatment (100 ng/mL) was evaluated by immunocytochemistry. The data from four independent experiments are presented as the mean ± SEM in (**A**), (**B**) and (**E**) – (**G**). *$p < 0.05$ vs. control samples in (**A**), (**B**) and (**E**) – (**G**); analysis of variance (ANOVA) with Bonferroni's test. Scale bars, 20 μm in (**D**) and (**H**).

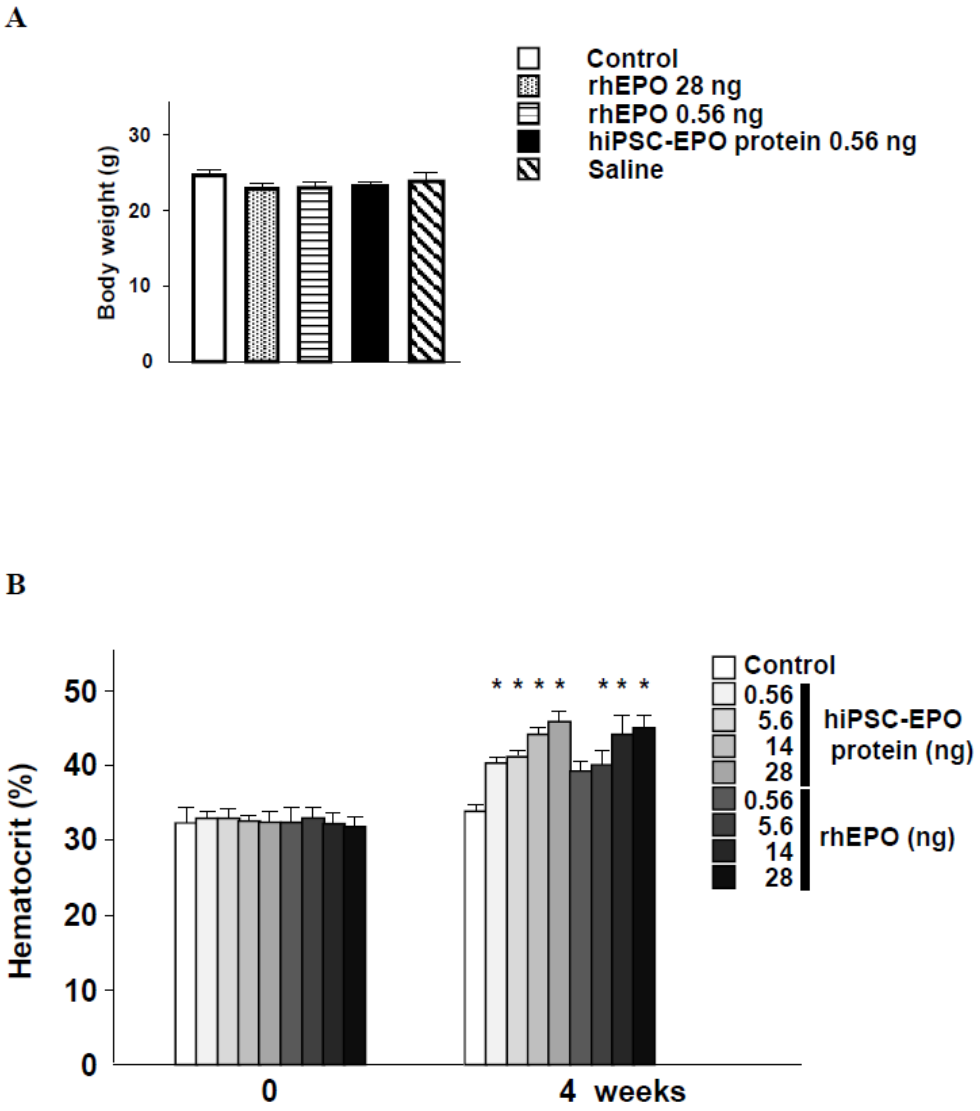

Fig. S7. Effects of hiPSC-EPO protein on body weight and renal anemia in adenine-treated mice.

(**A**, **B**) Renal anemia was induced using adenine treatment (50 mg/kg body weight daily for 4 weeks) in male C57BL/6 mice. The mice were treated with rhEPO or hiPSC-EPO protein. (**A**) The body weights of the mice after four weeks of treatments. (**B**) Hct levels after four weeks of treatments with different doses of rhEPO or hiPSC-EPO protein. The data from three independent experiments are presented as the mean ± SEM, n = 6. *p < 0.05 vs. control in (**B**); analysis of variance (ANOVA) with Bonferroni's test.

Supplementary Table S1. Effects of hiPSC-EPO protein on *in vitro* erythropoiesis (Related to Figure 6).

	CFU-GM	BFU-E	Mix
(-)	1.00 ± 0.58	0.00 ± 0.00	0.33 ± 0.33
ST3	6.00 ± 1.16	2.00 ± 0.00	5.33 ± 0.33
ST3+rhEPO			
0.28 ng/mL	7.00 ± 1.73	4.00 ± 0.58	5.33 ± 1.20
2.8 ng/mL	10.33 ± 2.33	6.67 ± 0.33 *	7.33 ± 1.20
ST3+hiPSC-EPO protein			
0.28 ng/mL	7.33 ± 1.67	5.33 ± 1.45	4.67 ± 1.20
2.8 ng/mL	9.33 ± 1.45	7.33 ± 1.20 *	6.00 ± 1.53
+ EPO antibody (μg/mL)			
0	5.00 ± 2.73	2.33 ± 1.67	3.67 ± 1.20
0.75	5.33 ± 1.67	2.00 ± 1.73	2.00 ± 2.00
1.5	3.67 ± 1.20	2.33 ± 0.67	2.67 ± 1.67
3.0	6.33 ± 0.33	0.67 ± 1.20	1.00 ± 1.00

The number of clonally emerged colonies on semi-solid medium containing stem cell factor, thrombopoietin and interleukin 3 (ST3) supplemented with 0.28 and 2.8 ng/mL of rhEPO or hiPSC-EPO protein is shown. The number of colonies on semi-solid medium containing different doses of neutralizing antibodies against human EPO in addition to ST3 and 2.8 ng/mL of hiPSC-EPO protein was also counted. The data from three independent experiments are presented as the mean ± SEM. *$p < 0.05$ vs. medium containing ST3 without EPO; analysis of variance (ANOVA) with Bonferroni's test.

Supplementary Table S2. The sequences of sense and antisense primers used for RT-PCR in this study.

Gene	Orientation	Primer sequence (5'-3')	Gene Bank association No
EPO	Sense	AGAATATCACTGTCCCAGACACC	NM000799
	Antisense	CCCCGGAGGAAATTGGAGTA	
(qRT-PCR)	Sense	TGTGGATAAAGCCGTCAGTG	
	Antisense	GATTGTTCGGAGTGGAGCAG	
Epo	Sense	TCCCACCCTGCTGCTTTTAC	NM007942
	Antisense	TCGTGACATTTTCTGCCTCC	
SOX17	Sense	CAGCAGAATCCAGACCTGCA	NM022454
	Antisense	GTCAGCGCCTTCCACGACT	
AFP	Sense	AAATGCGTTTCTCGTTGC	NM001134
	Antisense	GCCACACGGCCAATAGTTTGT	
ALB	Sense	CGCTATTAGTTCGTTACACCA	NM000477
	Antisense	TTTACAACATTTGCTGCCCA	
HIF1α	Sense	CCATTAGAAAGCAGTTCCGC	NM001530
	Antisense	TGGGTAGGAGATGGAGATGC	
HIF2α	Sense	GAAGTCCCGGGATGCTGCGCG	NM001430
	Antisense	ACTATGTCCTGTTAGCTCCAC	
HIF3α	Sense	TGTGACCAAGAGGAGCTTCAG	NM152794
	Antisense	TGTACTCTTCATGCGCAAGG	
HIF1β	Sense	AACCTCACTTCGTGGTGGTC	NM001668
	Antisense	CAATGTTGTGTCGGGAGATG	
HIF2β	Sense	GCAGGATGAGGTGTGGAAAT	NM014862
	Antisense	CACATCAGCGTCTTCTTCAG	
PHD1	Sense	AGCGGGCAGCAGCCAAAGACAAG	NM053046
	Antisense	TGCCATGCGGCTCTGGGACTG	
PHD2	Sense	AGCCCGGCTGCGAAACCATTG	NM022051
	Antisense	TTCGTCCGGCCATTGATTTTGT	
PHD3	Sense	AGATGTGGAGCCCATTTTTG	NM022073
	Antisense	CAGATTTCAGAGCACGGTCA	
β-ACTIN	Sense	CAATGTGGCCGAGGACTTTG	NM001101
	Antisense	CATTCTCCTTAGAGAGAAGTGG	
Gapdh	Sense	AACTTTGGCATTGTGGAAGG	NM001289726
	Antisense	GGATGCAGGGATGAGTTCT	

Supplementary Table S3. A list of lectins and their specificity for microarray analysis.

Lectin (origin)	Reported glycan selectivity
LTL (Lotus tetragonolobus)	Fucα1-3(Galβ1-4)GlcNAc (Lewis x), Fucα1-2Galβ1-4GlcNAc (H-type 2)
PSA (Pisum sativum)	Fucα1-6GlcNAc (Core Fuc) , α-Man
LCA (Lens culinaris)	Fucα1-6GlcNAc (Core Fuc), α-Man
UEA-I (Ulex europaeus)	Fucα1-2Galβ1-4GlcNAc (H-type 2)
AOL (Aspergillus oryzae)	Fucα1-6GlcNAc (Core Fuc), Fucα1-2Galβ1-4GlcNAc (H-type 2)
AAL (Aleuria aurantia	Fucα1-3(Galβ1-4)GlcNAc (Lewis x), Fucα1-6GlcNAc (Core Fuc),
MAL_I (Maackia amurensis)	Siaα2-3Galβ1-4GlcNAc
SNA (Sambucus nigra)	Siaα2-6Gal/GalNAc
SSA (Sambucus sieboldiana)	Siaα2-6Gal/GalNAc
TJA-I (Trichosanthes japonica)	Siaα2-6Gal/GalNAc, HSO3(-) -6Gal b1-4GlcNAc
PHAL (Phaseolus vulgaris)	tri/tetra-antennary complex-type N-glycan
ECA (Erythrina cristagalli)	Galβ1-4GlcNAc (up with increasing the number of terminal Gal), no affinity for fully sialylated N-type, fully agalactosylated N-type
RCA120 (Ricinus communis)	Galβ1-4GlcNAc (up with increasing the number of terminal Gal), Galb1-3Gal (weak), no affinity for agalactosylated N-type
PHAE (Phaseolus vulgaris)	bi-antennary complex-type N-glycan with outer Gal and bisecting GlcNAc, no affinity for fully sialylated N-type
DSA (Datura stramonium)	(GlcNAcβ1-4)n (Chitin), tri/tetra-antennary N-glycan
GSL-II (Griffonia simplicifolia)	agalactosylated tri/tetra antennary glycans, GlcNAc, no affinity for fully galactosylated or sialylated N-type
NPA (Narcissus pseudonarcissus)	High-Mannose including Manα1-6Man
ConA (Canavalia ensiformis)	High-Mannose including Manα1-6(Manα1-3)Man
GNA (Galanthus nivalis)	High-Mannose including Manα1-3Man
HHL (Hippeastrum hybrid)	High-Mannose including Manα1-3Man or Manα1-6Man
ACG (mushroom, Agrocybe cylindracea)	Gal b1-3Gal, Siaα2-3Galβ1-4GlcNAc
TxLCI (Tulipa gesneriana)	Manα1-3(Manα1-6)Man, bi/tri-antennary complex-type N-glycan, GalNAc
BPL (Bauhinia purpurea)	Galβ1-3GalNAc (up with Lewis x, down with Core Fuc), GalNAc
TJA-II (Tanthes japonica)	Fucα1-2Galβ1-> or GalNAcβ1-> groups at their non-reducing terminals

EEL (Euonymus europaeus)	Gala1-3Galb1-4GlcNAc, Fuca1-2Galb1-3GlcNAc (H antigen)
ABA (fungus, Agaricus bisporus)	Galβ1-3GalNAc, GlcNAc
LEL (tomato, Lycopersicon esculentum)	(GlcNAcβ1-4)n (Chitin), (Galb1-4GlcNAc)n (polylactosamine)
STL (potato, Solanum tuberosum)	(GlcNAcβ1-4)n (Chitin) oligosaccharide containing GlcNAc and MurNAc
UDA (Urtica dioica)	GlcNAcβ1-4GlcNAc (Chitin), High-Mannose (3 to High, up with increasing the number of Man)
PWM (pokeweed, Phytolacca Americana)	(GlcNAcβ1-4)n (Chitin)
Jacalin (Artocarpus integrifolia)	GlcNAcb1-3GalNAc (Core3), Siaa2-3Galb1-3GalNAc (sialyl T), Galb1-3GalNAc (T-antigen), a-GalNAc (Tn-antigen)
PNA (peanut, Arachis hypogaea)	Galβ1-3GalNAc
WFA (Wisteria floribunda)	GalNAcβ1-4GlcNAc (LacdiNAc), Galβ1-3(-6)GalNAc
ACA (Amaranthus caudatus)	Galβ1-3GalNAc (T-antigen), Siaa2-3Galb1- GalNAc (sialyl T)
MPA (Maclura pomifera)	a-GalNAc (Tn-antigen), Galβ1-3GalNAc (T-antigen),
HPA (snail, Helix pomatia)	α-GalNAc
VVA (Vicia villosa)	GalNAcb1-4Gal, GalNAcb1-3Gal, a-GalNAc,
DBA (Dolichos biflorus)	Blood group A, GalNAcα1-3GalNAc, GalNAcb1-4(Siaa2-3)Galb1-4Glc (GM2)
SBA (soybean, Dolichos biflorus)	α- or β-linked GalNAc, Gala1-4Gal-Glc
Calsepa (Calystegia sepium)	Galactosylated bianntenary N-type with bisecting GlcNAc (galacto > agalacto, down with Core Fuc), High-Mannose (Man2–6)
PTL-I (Psophocarpus tetragonolobus)	α-GalNAc, Gala1-3(Fuca1-2)Gal (B-antigen)
MAH (Maackia amurensis)	Siaα2-3Galβ1-3(Siaα2-6)GalNAc (disialyl-T)
WGA (wheat germ, Triticum aestivum)	(GlcNAcβ1-4)n (Chitin), Hybrid type N-glycan, Sia
GSL-I A4 (Griffonia simplicifolia)	α-GalNAc,
GSL-I B4 (Griffonia simplicifolia)	α-Gal,